Université de Montréal

14-3-3zeta is required for PKA-dependent lipolysis in mature adipocytes

Par

Abel Oppong

Faculté de médecine

Mémoire présenté à la Faculté des études supérieures

en vue de l'obtention du grade de Maître *es* science (M.sc)

en Sciences Biomédicales

option médecine expérimentale

Août, 2019

Université de Montréal

Faculté des études supérieures

Ce mémoire intitulé :

14-3-3zeta is required for PKA-dependent lipolysis in mature adipocytes

Présenté par :

Abel Oppong

A été évalué par un jury composé des personnes suivantes

Dr Mathieu Ferron

Président-rapporteur

Dr Gareth Lim

Directeur de recherche

Dre Julie Lavoie

Membre du jury

Résumé

Une augmentation de l'hypertrophie et l'hyperplasie des adipocytes est au cœur du développement de l'obésité. Nous avons déjà constaté que 14-3-3zeta (14-3-3ζ), une protéine d'échafaudage moléculaire, a plusieurs rôles essentiels dans l'adipogenèse. Cependant, les contributions de 14-3-3ζ dans la fonction des adipocytes matures ne sont pas connues. Les cellules 3T3-L1 et souris dépourvues de 14-3-3ζ dans les adipocytes (adi14-3-3ζKO) ont été utilisés pour examiner le rôle de 14-3-3ζ dans la lipolyse. L'élimination de 14-3-3ζ dans les cellules 3T3-L1 par l'ARNi a réduit significativement la lipolyse stimulée par l'isoprotérénol (un agoniste bêta adrénergique), la forskoline (un activateur de l'adénylate cyclase) et le dibutyryl AMPc (dbcAMP). Les analyses par qPCR ont démontré des réductions significatives d'*adipose triglyceride lipase* (*Atgl)* et *lipase hormonsensible* (*Hsl*) au niveau transcriptionnel. De plus, une réduction au niveau des substrats de la PKA phosphorylés et totaux tels que HSL et CREB, a été détectée par Western Blot dans les 3T3-L1 appauvris en 14-3-3ζ. Ces résultats in vitro ont été récapitulés *in vivo*, car des diminutions des taux phosphorylés et totaux de HSL ont été observés dans le tissu adipeux gonadique des souris adi14-3-3ζKO. Les souris adi14-3-3ζKO et les explants gonadiques ont également montré une lipolyse affaiblie après des injections i.p de l'agoniste bêta 3-adrénergique CL-316,243 et un traitement de l'isoprotérénol respectivement. De manière intéressante, une diminution de l'expression de 14-3-3ζ dans les cellules 3T3-L1 et les souris adi14-3-3ζKO a mené à une diminution des caractéristiques des adipocytes matures telles que les niveaux d'ARNm de *Pparg, Lpl* et *Fabp4*, les niveaux de PPARγ, le contenu en triglycérides et l'incorporation de Oil Red-O. Collectivement, ces résultats démontrent que 14-3-3ζ joue un rôle essentiel en facilitant la lipolyse et en déterminant la maturité des adipocytes.

Mots-clés : lipolyse, lipase, adipocyte mature

Abstract

Altered hypertrophy and hyperplasia of adipocytes lie at the core of the development of obesity. We previously demonstrated that the molecular scaffold 14-3-3zeta (14-3-3ζ) had essential roles in adipogenesis. However, the contributions of 14-3-3ζ to mature adipocyte function are not known. 3T3-L1 cells and tamoxifen-inducible adipocyte-specific 14-3-3ζ knockout mice (adi14-3-3ζKO) models were used to examine the roles of 14-3-3ζ in lipolysis. siRNA-mediated knockdown of 14-3-3ζ impaired lipolysis in 3T3-L1 cells stimulated by the beta-adrenergic agonist isoproterenol (Iso), forskolin (an activator of adenylyl cyclase) and dibutyryl cAMP (dbcAMP). qPCR analyses revealed significant reductions in lipase transcript levels *(Atgl* and *Hsl*). Furthermore, reductions in the phosphorylated and total levels of PKA substrates such as HSL and CREB were detected in 14-3-3ζ-depleted 3T3-L1 lysates by immunoblotting. These findings were recapitulated *in vivo,* as reductions in phosphorylated and total HSL levels were detected in the gonadal adipose tissue of adi14-3-3ζKO mice. adi14-3-3ζKO mice and gonadal explants also displayed impaired lipolysis following *i.p* CL-316,243 (a beta-3 adrenergic agonist) injections and Iso treatment respectively. Interestingly, decreased 14-3-3ζ expression in 3T3-L1 cells and mice revealed reductions in characteristics of a mature adipocyte, such as *Pparg, Lpl,* and *Fabp4* transcript levels, PPARγ levels, triglyceride content, and Oil Red O (ORO) incorporation. Collectively, these results demonstrate that 14-3-3ζ has essential roles in facilitating lipolysis and determining adipocyte maturity.

Keywords: lipolysis, lipase, mature adipocyte

Table of Contents

List of Tables

1.0 Introduction

2.0 Research Article

List of Figures

1.0 Introduction

2.0 Research article

List of abbreviations

ACC	Acetyl-CoA carboxylase
ACLY	ATP-citrate lyase
adi14-3-3ζKO	Adipocyte-specific 14-3-3ζ knockout mice
Adrb	Adrenergic β-receptor
APC	Adipocyte precursor cell
ATGL	Adipose triglyceride lipase
ATP	Adenosine triphosphate
BAD	Bcl-2-associated death promoter
BAT	Brown adipose tissue
BMP	Bone morphogenic protein
CDC25B	Cell division cycle 25B
C/EBP	CCAAT/enhancer-binding protein
cAMP	Cyclic adenosine monophsophate
ChREBP	Carbohydrate-response element binding protein
CREB	cAMP-responsive element binding protein
CTBP	C-terminal binding proteins 1 and 2
dbCAMP	Dibutyryl cyclic adenosine monophosphate
DLK	Delta-like-1
DPP4	Dipeptidyl peptidase 4
FACS	Fluorescence activated cell sorting
FAP	Fibro-adipogenci precursor
FASN	Fatty acid synthase
FFA	Free fatty acids
GAPDH	Glyceraldehyde-3-phosphate dehydrogenase
GLUT4	Glucose transporter
GPCR	G-protein coupled β-adrenergic receptor
gWAT	Gonadal white adipose tissue
HFD	High-fat diet
HSL	Hormone sensitive lipase
IBMX	Isobutylmethylxanthine
IKK	Inhibitor of κβ

IPC	Interstitial progenitor cell
IPGTT	Intraperitoneal glucose tolerance test
ITT	Intraperitoneal insulin tolerance test
JNK	JUN N-terminal kinase
KLF	Kruppel-like factor
MAGL	Monoacylglycerol lipase
MAPK	Mitogen-activated protein kinase
MSC	Mesenchymal stem cell
ORO	Oil Red-O
PDGF	Platelet-deteived growth factor
PFK-2	Phosphofructo-2-kinase/fructose-2,6-biphosphatase
PGC-1	Peroxisome proliferator-activated receptor gamma co-activator
PKA	Protein kinase A
PKB	Protein kinase B
PKC	Protein kinase C
PLIN1	Peripilin 1
PPAR	Peroxisome proliferator-activated receptor
PRDM16	PRD1-BF1-RIZ1 homologous domain-containing 16
PREF	Pre-adipocyte factor
qPCR	quantitative polymerase chain reaction
ROCK	Rho-associated kinase
SCD-1	Stearoyl-CoA desaturase
scRNAseq	single cell RNA sequencing
SREBP	Sterol response element binding protein
SVF	Stromal vascular fraction
TCA	Tricarboxylic acid (TCA)
TGF-β	Transforming growth factor-beta
UCP1	Uncoupling protein 1
WAT	White adipose tissue
WNT	Wingless-type MMTV integration site signaling
YWHA	Tyrosine- and tryptophan-hyroxylase activator

Acknowledgements

I would first like to thank my research supervisor Dr. Gareth Lim for giving me the opportunity to do my master's project in his laboratory. I thank him for his extensive support as a mentor who devoted countless hours to ensure that I could succeed in realizing this research project. I truly appreciate his mentoring approach over the last two years which included personally walking me through some experiments and readily making himself available for discussions about the current literature and my progress.

I also would like to thank Dr. Mathieu Ferron and Dr. Julie Lavoie for agreeing to evaluate my dissertation. I also want to thank them for the critiques and suggestions they gave while also being members of my Advisory Committee earlier during Graduate studies.

I would also like to thank my fellow lab members Dr. Yves Mugabo and Kadidia Diallo for their assistance and suggestions for improving and troubleshooting experiments. I could not ask for a better group of lab members to work with. I particularly want to thank Dr. Mugabo for being an exceptionally patient mentor who assisted and trained me with handling mice despite me having no prior experience with working with animals.

Finally, I would like to thank my parents and my sister Isabelle for their love and constant support throughout this journey.

1.0 Introduction

1.1 Overview of adipocyte development and function

1.1.1 Adipogenesis

Adipogenesis is the process whereby pluripotent mesenchymal stem cells (MSCs) develop into mature adipocytes and consists of two phases: commitment to a cell lineage (or determination), and terminal differentiation. During adipogenesis, mesenchymal stem cells that undergo determination are committed to becoming pre-adipocytes and lose the ability differentiate into other cell types. The pre-adipocytes then differentiate into mature adipocytes and gain features necessary for lipid synthesis, hydrolysis and transport, glucose uptake, insulin sensitivity and adipokine secretion (Figure 1) [1].

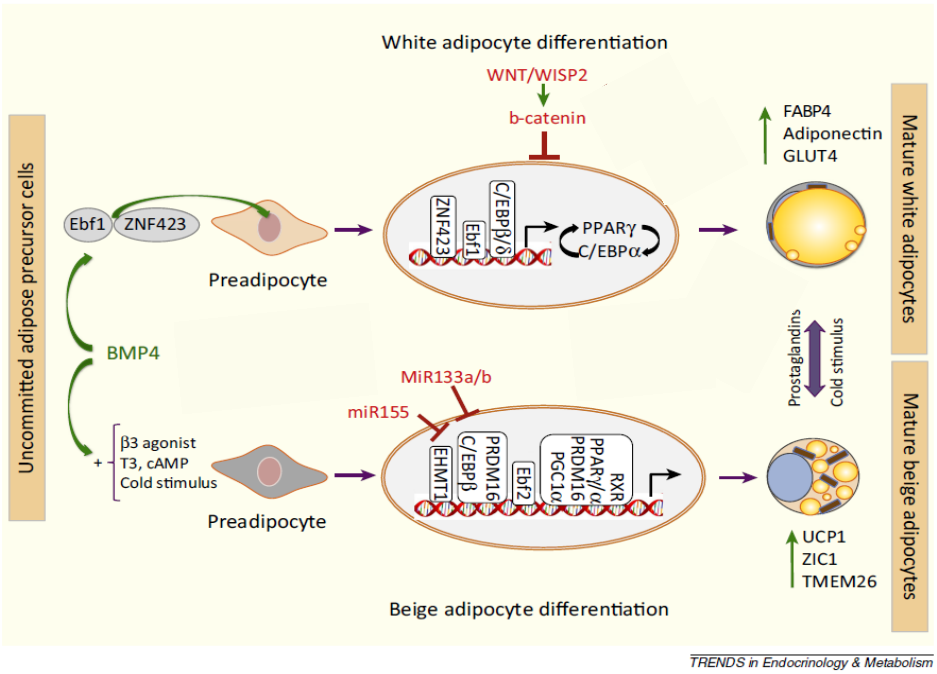

Figure 1: Overview of adipogenesis. Commitment of mesenchymal stem cells (MSCs) to the adipocyte lineage is mediated by factors such as bone morphogenetic protein 4 (BMP4). In contrast, β-catenin-dependent Wingless-type MMTV integration site (WNT) signaling inhibits the conversion of MSCs into pre-adipocytes by inhibiting the expression of the master transcription factors Peroxisome proliferator-activated receptor gamma (PPARγ) and CCAAT/enhancer-binding protein alpha (C/EBP-α). These transcription factors are induced by C/EBP-β and C/EBP-δ which are expressed during early adipogenesis. Terminal differentiation is driven by PPARγ and C/EBP-α promoting each other's expression in a positive feedback loop and results in the induction of mature adipocyte genes such as *FABP4*, adiponectin and *GLUT4*. The transcription factor PRD1-BF1-RIZ1 homologous domain-containing 16 (PRDM16) associates with PPARγ coactivator 1 alpha (PGC1α) to promote the expression of thermogenic genes such as *UCP1* and mediates the browning of white adipocytes that is induced by β3 agonists and cold exposure. The roles of the abovementioned factors and others in the regulation of adipogenesis are further discussed in the text below. Figure taken and modified from [2].

While MSCs mainly originate from bone marrow, they are also found in other organs, such as fat, lung, and skin [3]. MSCs are multipotent in that they can develop into precursors of multiple specialized cells, including adipocytes, myocytes, chondrocytes, and osteoblasts [4]. Specialized cells can be categorized by the presence or absence of proteins in precursor cells that they originate from. For instance, brown adipocytes and myocytes derive from *Myf5*$^{+}$ precursor cells whereas white and beige adipocytes and osteocytes derive from *Myf5*$^{-}$ precursor cells [5]. Lineage commitment of MSCs is also

regulated by several signaling pathways including Wingless-type MMTV integration site (WNT), transforming growth factor-beta/bone morphogenic protein (TGF-β/BMP) signaling, Notch, and Hedgehog. (Figure 2)

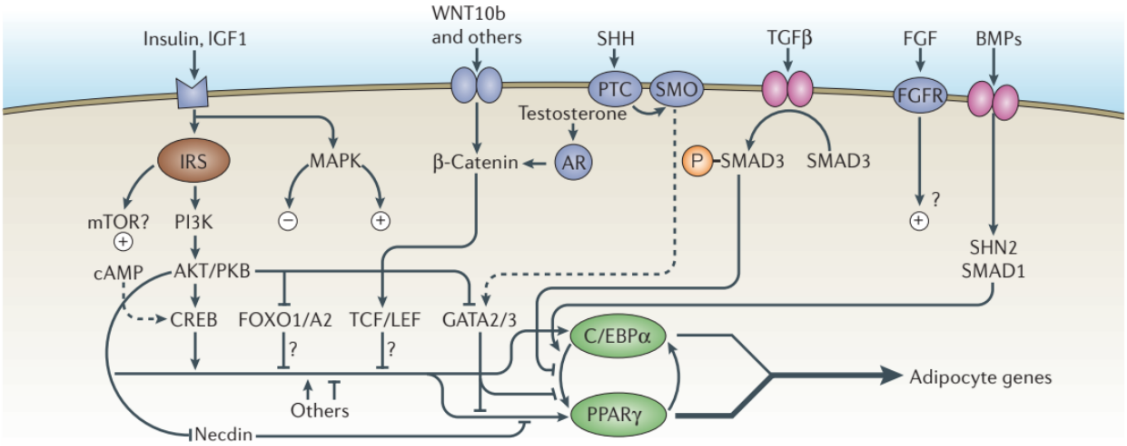

Figure 2: Signaling pathways involved in the regulation of adipogenesis. Signaling pathways affect adipogenesis by activating downstream transcription factors that promote or inhibit the expression of Peroxisome Proliferator-Activated Receptor gamma (PPARγ) and CCAAT/Enhancer-Binding Protein alpha (C/EBP-α). Signaling pathways that negatively regulate adipogenesis include Wingless-type MMTV integration site (WNT), transforming growth factor-beta (TGF-β), and sonic hedgehog (SHH). In the canonical WNT pathway, β-catenin recruits the transcription factor T cell factor (TCF) to activate WNT targets that inhibit adipogenesis. The transcription factors GATA2/3 and SMAD3, which are downstream of the SHH and TGF-β pathways respectively, inhibit adipogenesis by hindering C/EBP-α from binding to the *Pparg* promoter. Conversely, bone morphogenetic protein (BMP)2/4 promote adipogenesis through the activation of the transcription factor SMAD1. The transcription factor cyclic AMP (cAMP) response element-binding protein (CREB) promotes the transcription of C/EBP-β which in turn induces PPARγ expression during early adipogenesis. Image taken from [1].

WNT belongs to a family of glycoproteins that regulates MSC fate to either adipocyte or osteoblast lineages. In the case of canonical (β-catenin-dependent) signaling, WNT ligands like WNT10β promote the nuclear translocation of β-catenin, resulting in the activation of WNT target genes that promote osteogenic differentiation and inhibits adipogenic differentiation via the suppression of the adipogenic master regulators, PPARγ and C/EBP-α [3] (Figure 2). In contrast, WNT-5β, a non-canonical WNT ligand promotes adipogenesis by inhibiting WNT10β-mediated signaling possibly through ROR receptors [3, 6]. The TGF-β family of secreted ligands have regulatory roles in cell proliferation and cell

differentiation [3]. This family is divided into 3 sub-types: TGFβ1-3, with BMPs belonging in the TGFβ1 sub-family. TGFβ/BMPs regulate adipogenic and osteogenic MSC differentiation through both the activation of SMAD transcription factors and SMAD-independent pathways such as the p38 mitogen-activated protein kinase (MAPK) pathways. Several BMPs including BMP2 and BMP4 are associated with promoting adipogenic differentiation of MSCs (Figure 2) [7, 8].

The Notch family of transmembrane proteins has also been implicated in regulating adipogenic differentiation of MSCs. Ross et al. showed that the Notch ligand Jagged1 blocks PPARγ and C/EBP-α expression in 3T3-L1 cells, a fibroblast cell line derived from Swiss 3T3 mouse embryos that can differentiate into adipocytes [9]. Another study demonstrated that inhibition of Notch via the PI3K/AKT/mTOR pathway promotes autophagy-mediated adipogenic differentiation of MSCs [10]. Lastly, hedgehog secretory proteins have also been reported to induce osteogenic differentiation and inhibit adipogenesis in MSCs by decreasing *PPARG* and *C/EBPA* expression through GLI transcription factors [11].

Terminal differentiation is controlled by several transcription factors that temporally regulate a series of metabolic and adipokine gene-expression events. Induction and maintenance of this transcriptional cascade is primarily driven by the expression and interactions of two crucial transcriptional regulators: Peroxisome Proliferator-activated Receptor gamma (PPARγ) and CCAAT/Enhancer-Binding Protein (C/EBP). PPARγ is a ligand-activated transcription factor that belongs to the superfamily of hormone nuclear receptors. PPARγ exists as two isoforms in mice, PPARγ1 and PPARγ2. These isoforms differ in that the N-terminal region of PPARγ2 contains an additional 30 amino acids compared to PPARγ1. In contrast to PPARγ1 which is expressed in multiple tissues, PPARγ2 expression is adipocyte-specific. Upon activation by endogenous ligands (fatty acids such as nitrolinoleic acid), PPARγ forms a heterodimer with retinoid X receptor and binds to specific PPAR response element

regions of target genes involved in lipogenesis, lipolysis, and adipogenesis to increase the expression of their corresponding proteins, including FABP4, LPL, perilipin, and glycerol kinase [12].

Several *in vivo* models have demonstrated the role of PPARγ as a master regulator of adipogenesis. One of the earliest reports came from Barak et al. who generated chimeric *Pparg* knockout mice by supplementing knockout embryos with wild-type tetraploid cells to rescue the *Pparg* knockout mice from an embryonic lethal phenotype [13]. The absence of BAT and WAT in the chimeric mutants suggested that PPARγ was required for adipogenesis. In another study, systemic deletion of PPARγ2 yielded severely lipodystrophic mice with virtually no WAT and smaller BAT. Growth retardation accounted for nearly half of these mice dying before reaching adulthood. Furthermore, compensation by muscle to consume excess lipids limited the extent of metabolic dysfunction in these mice as they were mildly glucose intolerant and did not develop fatty livers [14]. In a recent study, Wang and colleagues observed that adipocyte-specific PPARγ knockout mice had almost no visible WAT or BAT at 3 months of age. These lipodystrophic mice also displayed severe metabolic phenotypes including insulin resistance, fatty liver and abnormalities in tissues that normally contain WAT such as bone and mammary glands [15].

CCAAT/enhancer-binding proteins (C/EBPs) are a class of transcription factors that contain a basic leucine zipper domain. Among the 6 isoforms (α, β, δ, γ, ε, and ζ) comprising this family, C/EBP-α, C/EBP-β, and C/EBP-δ play key roles in stimulating adipogenesis. C/EBP-β and C/EBP-δ are maximally expressed during early adipogenesis and bind to the *Pparg* promoter to induce PPARγ expression [6]. Transcriptional regulation of C/EBP-β is mediated by factors including cAMP-responsive element binding protein (CREB) and STAT3, whereas MAPK and GSK3β regulate C/EBP-β phosphorylation which is required for C/EBP-β binding to DNA [16]. While CEBP-δ expression was reported to be induced by glucocorticoids [17], little is known about C/EBP-δ regulation. C/EBP-α expression is later induced by PPARγ and participates in a positive-feedback loop with PPARγ by reciprocally binding to the PPARγ

promoter to reinforce PPARγ expression and drive adipogenesis (Figure 2) [18, 19]. *In vivo* models have also demonstrated the contributions of C/EBPs to adipogenesis. For instance, transgenic mice lacking C/EBP-α in all tissues except the liver had almost no subcutaneous, perirenal and epididymal WAT although fat was present in mammary glands. These mice also had elevated lipid levels in the serum [20]. In another study, global, double knockout mice that lacked C/EBP-β and CEBP-δ displayed reduced lipid accumulation in BAT and significantly reduced epididymal fat depots despite expressing normal levels of PPARγ and C/EBP-α [21]. This demonstrates that the induction of PPARγ and C/EBP-α alone is not enough for complete adipocyte differentiation to occur.

Other transcription factors contribute to the regulation of adipogenesis by promoting or inhibiting the expression and activity of PPARγ and C/EBP-α proteins. Kruppel-like factors (KLFs) are zinc-finger proteins that have established roles in regulating differentiation, proliferation and apoptosis [6]. The KLF family consists of both pro-adipogenic and anti-adipogenic members. KLFs that promote differentiation include KLF5, KLF6, and KLF15, whereas KLF2 and KLF7 inhibit adipogenesis. Upon induction by C/EBP-β and C/EBP-δ, KLF5 binds and activates the *Pparg* promoter to maintain the differentiated state [22]. The role of KLF5 in adipogenesis was recapitulated *in vivo* by Oishi and colleagues who showed that heterozygous KLF5 knockout mice displayed impaired WAT development within the first few days after birth [22]. Heterozygous mice also weighed less than control littermates. In addition, WAT depots from the back and neck were significantly smaller and adipocytes contained either smaller or no lipid droplets compared to wild-type adipocytes.

KLF6 promotes adipogenesis in 3T3-L1 cells by inhibiting the expression of delta-like-1/pre-adipocyte factor-1 (DLK1/PREF-1), a transmembrane protein that inhibits adipocyte differentiation by activating the ERK/MAPK pathway to stimulate SOX9 expression [23]. In addition to promoting adipocyte differentiation, KLF15 also induces the expression of glucose transporter 4 which is necessary for insulin-mediated glucose uptake. In contrast, KLF2 inhibits adipogenesis by repressing the *Pparg*

promoter [24]. Similarly, KLF7 decreases PPARγ and C/EBP-α expression [25]. GATA transcription factors also contain zinc finger domains and regulate cellular processes, such as proliferation and differentiation, by binding to specific DNA sequences. GATA proteins such as GATA2 and GATA3 inhibit adipogenesis by directly binding to the *Pparg* promoter or by binding to C/EBP-α to decrease its transcriptional activity on the *Pparg* promoter [26].

In contrast to white adipogenesis, PPARγ and C/EBPs have less prominent roles in the differentiation of brown adipocytes when compared to the transcription factor PRD1-BF1-RIZ1 homologous domain-containing 16 (PRDM16), which was shown to be crucial to brown adipogenesis. In fact, PRDM16 was reported to act as a molecular switch controlling the fate of *Myf5*$^{+}$ precursor cells between brown adipocyte and myocyte lineages [27]. While PRDM16 participates in the induction of adipocyte-related genes such as *Pparg* and *Fabp4*, it also induces the expression of brown adipocyte-specific and thermogenic genes, such as *Ucp1* upon forming a transcriptional complex with C/EBP-β and PPARγ [6]. PRDM16 also associates with PPARγ co-activator 1α (PGC-1α) to induce the expression of genes related to mitochondrial biogenesis and adaptive thermogenesis in brown adipocytes [4]. In addition, PRDM16 inhibits the expression of white adipocyte genes, such as resistin and angiotensinogen, by forming a transcriptional repression complex with C-terminal binding proteins 1 and 2 (CTBP1 and CTBP2) [28]. PRDM16 is also expressed in white adipocytes and plays a role in mediating the browning or "beiging" of white adipocytes stimulated by cues such as β3-adrenergic stimulation and cold exposure [29].

1.1.2 General functions of adipocytes

The regulation of energy homeostasis is principally mediated by three types of adipocytes: white, brown and beige. These adipocytes differ in several aspects, including morphology, function, and gene expression. White adipocytes are the principal component of white adipose tissue (WAT) which

specializes in the storage of lipids. White adipocytes have unilocular lipid droplets and few mitochondria. In contrast, brown adipocytes specialize in thermogenesis and contain multilocular lipid droplets and a high density of mitochondria [30]. Brown adipocytes dissipate energy in the form of heat by the action of uncoupling protein 1 (UCP-1), which uncouples the electrochemical proton gradient from ATP production. Beige adipocytes are interspersed within WAT and acquire brown adipocyte-like features under conditions, such as cold stimulation and β3 adrenergic receptor stimulation [31]. In the basal state, beige adipocytes resemble white adipocytes; however, upon stimulation, beige adipocytes acquire the brown adipocyte phenotype, as both mitochondrial density and UCP-1 expression increase [32]. Removal of stimuli reverses the browning process thereby returning beige adipocytes back to the basal state [33].

The functions of adipose tissue extend beyond regulating lipid storage and energy dissipation as they also include protecting delicate organs such as the eye, protecting body parts from mechanical stress, moving skeletal components within joints, and sculpting facial features [5, 34]. Since the discovery of leptin, adipose tissue has been recognized as a major endocrine organ involved the regulation of whole-body glucose metabolism, systemic insulin sensitivity, and inflammatory responses [35]. White adipocytes also secrete a wide range of cytokines (also called adipokines) that affect whole-body metabolism and regulate inflammation. Leptin, which is perhaps the most renowned adipokine, is secreted in proportion to adipose tissue mass and plays an important role in regulating food intake. One of the well-known functions of leptin includes its binding to leptin receptors in the hypothalamus to reduce appetite and food intake [36]. Upon binding to its cognate receptors, ADIPOR1 and ADIPOR2, adiponectin promotes insulin sensitivity in tissues, such as the liver and skeletal muscle, through crosstalk between the adiponectin and insulin signaling pathways. More specifically, an adaptor protein (APPL1) that is initially bound to ADIPOR1/2 mediates the action of adiponectin by binding to IRS1/2, which promotes IRS1/2 binding to the insulin receptor to ultimately enhance insulin signaling [37]. In

contrast, proinflammatory cytokines like resistin, tumor necrosis factor-α (TNF-α), and IL-6 contribute to insulin resistance by activating inflammation pathways involving c-Jun N-terminal kinase (JNK) and inhibitor of κβ (IKK) that result in increased serine phosphorylation of IRS molecules [38]. Other adipokines and their reported functions are listed in Table 1.

Table 1: Examples of adipokines secreted by WAT and BAT and their functions

Adipokine	Source	Function	Reference
Adiponectin	WAT	Insulin sensitization in peripheral tissues	[37]
BMP2/4/7	WAT, BAT	Regulation of commitment and differentiation of adipogenic precursor cells	[39] [40] [41]
IL6	WAT, BAT	Promotes inflammation, inhibits insulin signaling	[42, 43]
Leptin	WAT	Regulates appetite via central nervous system	[36]
MCP-1	WAT	Recruitment of monocytes to adipose tissue	[44]
NRG4	WAT, BAT	Maintains adipose tissue vasculature, regulates hepatic lipogenesis	[45] [46]
Resistin	WAT	Modulates glucose homeostasis by inhibiting insulin signaling	[47]
TNF-α	WAT	Promotes inflammation, inhibits insulin signaling	[48]
VEGF	WAT, BAT	Stimulates angiogenesis in adipose tissue	[49]

BMP, bone morphogenic protein; IL6, interleukin 6; MCP-1, moncocyte chemoattractant protein-1; NRG4, neuregulin 4; TNF-α, tumor necrosis factor alpha; VEGF, vascular endothelial growth factor

1.1.3 Interactions between adipocytes and other cell-types

Adipocytes have been shown to play additional roles in various biological processes through crosstalk with other cell types. In the context of obesity, elevated levels of proinflammatory adipokines promote the recruitment of monocytes to adipose depots to increase the inflammatory response and clear infections [50]. Macrophages are also recruited to adipose depots by free fatty acids (FFAs) during fasting and weight loss periods and take up nearby lipids to maintain circulatory free fatty acids levels [51]. In addition, M2 macrophages activated by cold exposure in an IL-4-dependent manner were shown to secrete catecholamines that promote the browning of white adipose tissue, confirming reciprocal crosstalk between macrophages and adipocytes [52]. Adipocyte progenitor cells were shown to promote

hair growth in mice by stimulating the expression of platelet-derived growth factor α (PDGF-α), which induces stem cell activation in hair follicles [5]. Adipocytes found in the epicardium are associated with increased atherosclerosis and blood pressure [53]. Furthermore, adipocytes regulate insulin sensitivity in skeletal muscle [54]. Adipocyte-myocyte interactions also involve fibro-adipogenic precursor (FAP) cells which exist in skeletal muscle and can differentiate into white adipocytes under conditions of metabolic dysfunction and muscular dystrophy. Undifferentiated FAPs were previously shown to be involved in muscle repair following muscle damage, whereby they proliferate, clear necrotic cells, and promote myogenesis in response to cytokine production at the site of injury [5].

Adipocytes in the bone marrow arise from multipotent precursor cells that commit to either the osteoblast or adipocyte lineages. This cell fate decision is thought to explain an inverse association between marrow fat and bone strength and density [55]. In addition, several studies have demonstrated reciprocal regulation between adipocytes and osteoblasts. For instance, Hamrick and colleagues reported that leptin-deficient ob/ob mice treated with leptin displayed a loss in the size and number of bone marrow adipocytes as well as increased bone formation [56]. In contrast, Luo et al. showed that adiponectin negatively regulates bone formation by inhibiting the production of the osteoclastogenesis inhibitor, osteoprotegerin, in osteoblasts [57]. Conversely, osteocalcin which is secreted by osteoblasts, was reported by Ferron and colleagues to affect fat mass and improve insulin sensitivity in wild-type mice by stimulating the release of adiponectin in white adipose tissue [58]. Adipocytes have also been implicated in tumor development, as one *in vitro* study demonstrated that leptin promotes tumor proliferation by activating the ERK1/2 and JNK pathways [59]. Secretion of cytokines such as IL-6 and MCP-1 promote macrophage recruitment to proinflammatory environments that are optimal for tumor proliferation [60]. Cytokines also mediate tumor migration and homing to adipose depots (e.g. omental depot) that provide cancer cells with fatty acids to serve as fuel for rapid cell division [59]. Additionally, adipocytes secrete ECM components such as collagen VI and matrix metalloproteinase 11 that promote

ECM remodelling [59]. Adipocytes also secrete VEGF-A which stimulates angiogenesis to accommodate the increased demand for nutrients and O_2 to be delivered at tumor sites [49].

The functional diversity of adipocytes is also reflected by the identification of adipocytes that are distinct from their traditional white, brown and beige counterparts. These include pink and yellow adipocytes that develop in mammary glands and in the bone marrow respectively. Mammary adipocytes are involved in the regulation of epithelial growth and epithelium function, and communicate with other cell types in mammary glands [61-63]. Lineage tracing studies by Cinti and colleagues led to the observation that subcutaneous adipocytes in mammary glands convert into milk-secreting epithelial cells [64]. In this regard, mammary adipocytes were reported to dedifferentiate into fibroblast-like preadipocytes during lactation to allow for mammary alveolar structures to expand and develop milk-secreting properties in the ductal epithelium of the mammary gland [65, 66]. However, these findings were recently challenged in a report by Wang et al. who used a doxycycline-inducible adipocyte-specific tracking model to demonstrate that mammary adipocytes do not trans-differentiate into milk-secreting alveolar cells [66]. During the involution period, these preadipocytes re-differentiate into mature mammary adipocytes as mammary alveolar structures undergo apoptosis [66-68].

Bone marrow adipocytes have unique features compared to adipocytes found in other depots. For instance, marrow adipocytes are smaller and differ in fatty acid composition compared to other adipocytes [69]. Lipid mobilization doesn't occur in marrow adipocytes during caloric restriction despite marrow adipocytes being able to hydrolyze lipids [70, 71]. In addition, progenitor cells of marrow adipocytes lack cell surface markers such as CD24 that are seen in progenitor cells for other adipose depots [55, 72]. Thus, the influence that adipocytes have on other cell types and tissues demonstrates that the function of adipose tissue is more complex than just regulating energy homeostasis.

1.1.4 Functional differences between different adipose depots

Adipose tissue can be further classified into depots according to their location. In the case of WAT, most depots are generally categorized as being visceral (vWAT) or subcutaneous (scWAT) tissue. In humans, vWAT includes the mesenteric, omental, retroperitoneal and epicardial depots. scWAT encompasses depots found in the abdominal, gluteal, and femoral regions. All vWAT depots listed above are also found in mice except for epicardial depots [73]. Conversely, epididymal fat depots that are present in mice are not found in humans [5]. vWAT and scWAT also differ in physiological and metabolic function. For instance, vWAT adipocytes are more metabolically active and insulin-resistant than scWAT [74, 75]. Visceral adipocytes also display greater lipolytic activity, as they are more sensitive to catecholamine-stimulated lipolysis, which is the hydrolysis of triglycerides into FFA and acylglycerols [31, 76]. Furthermore, inflammatory cells are more prevalent in vWAT compared to scWAT depots [77, 78]. scWAT depots are also more efficient in taking up FFA and triglycerides from circulation during the postprandial period [76]. These differences explain in part why vWAT is closely associated with insulin resistance, hyperglycemia, dyslipidemia and mortality in comparison to scWAT which is even associated with protection against cardiometabolic disease in obesity [31, 79]. In humans, BAT is distributed around the paravertebral, supraclavicular, and suprarenal regions in humans whereas in mice, BAT is divided into the interscapular and perirenal depots [73].

1.1.5 Heterogeneity of adipose tissue

Functional differences between adipose depots may result from heterogeneity among adipocyte precursor cells (APCs) that develop into different adipocyte populations. Methods such as lineage tracing, fluorescence activated cell sorting (FACS), and single-cell RNA sequence (scRNAseq) analysis have led to the identification of distinct APC populations and have advanced our understanding of the developmental origins of different adipose depots. One example is the case of Seale and colleagues who

used the Cre–LoxP system to investigate whether white and brown adipocytes shared a common precursor expressing *Myf5,* which was initially thought of being expressed solely in myocytes. Lineage tracing by Cre–LoxP is a method that uses reporter and Cre recombinase models to evaluate whether progeny cells express genes that are also expressed by precursor cells belonging to a specific lineage. White and brown adipocytes were determined to be derived from separate APCs that were *Pax7*$^{-}$*; Myf5*$^{-}$ and *Pax7*$^{+}$*; Myf5*$^{+}$ respectively [27, 80]. Furthermore, brown adipocytes and skeletal muscle were derived from a common precursor cell whose fate into either lineage was controlled by PRDM16 [27]. Lineage tracing also indicated that beige adipocytes that develop in WAT following stimulation with an β3-adrenergic agonist were not derived from *Myf5*$^{+}$ precursors of intrascapular BAT but did resemble *Myf5*$^{-}$ white adipocyte precursors [27].

In another study, Rodeheffer and colleagues used FACS, a technique that separates cells based on the absence or presence of cell-surface proteins, to characterize the preadipocyte lineage using APCs collected from the stromal vascular fraction (SVF) of murine adipose tissue. Rodeheffer et al. defined this population as being negative for CD31, CD45, and Ter119 which are respectively expressed in committed lineages for endothelial cells, macrophages and erythrocytes [30]. This population was positive for CD29, CD34, Sca1 and CD24 stem cell markers [81]. To confirm that adipocytes were derived from this population of cells, these precursor cells were transplanted into depots of lipodystrophic mice, and the successful reconstitution of WAT in these mice validated the identification of these precursor cells belonging to the adipocyte lineage [81]. In a later study, lineage tracing by the Cre–LoxP system was utilized to determine whether white adipocytes in mice could be derived from hematopoietic and endothelial lineages [82]. Results from that study indicated that WAT was not derived from either lineage, which was consistent with the earlier identification of an APC population by FACS that was devoid of endothelial and erythrocyte cell surface markers. Additional lineage tracing studies using *Pdgfra-Cre* mice led to the identification of adipocyte precursors that were either positive or negative

for the cell surface marker CD24. The expression of adipocyte-associated genes like *Pparg* and *C/ebpa* in $CD24^-$ APCs but not in $CD24^+$ APCs led Rodeheffer and colleagues to the conclusion that $CD24^+$ precursors develop into $CD24^-$ precursors that are more committed to the preadipocyte lineage [82]. Additional studies into the heterogeneous origins of WAT depots that utilized the lineage tracing by Cre–LoxP method demonstrated that APCs from respective depots originate from distinct areas of the mesoderm [30, 83, 84].

In a recent study conducted by Merrick et al., separation of fat cells with FACS followed by further grouping of cells by single-cell RNA sequencing (scRNAseq, a method that groups cells according to gene expression) led to the identification of three novel APC populations in mice and humans: interstitial progenitor cells (IPCs) expressing Dipeptidyl Peptidase-4 (DPP4), preadipocytes expressing intercellular adhesion molecule-1 (ICAM1), and group 3 cells expressing CD142 [85]. Based on *in vivo* cell transplantation studies, DPP4-expressing IPCs are progenitor cells for committed ICAM1- and CD142-expressing preadipocytes. Merrick et al. noted that group 3 APCs are present in the subcutaneous fat of mice but not humans. The idea of APC heterogeneity contributing to differences between adipose depots was supported by the finding that fewer IPCs were present in visceral depots than in subcutaneous depots [85]. Adipocyte heterogeneity has not only been seen between different depots, but also among adipocytes within a single depot. Reports of mature white adipocytes isolated from a single depot displaying variable lipogenesis, insulin sensitivity and fatty acid uptake suggest that a single adipose depot may be comprised of several distinct adipocyte subtypes [86, 87]. Furthermore, Lee et al. utilized *in* vitro clonal cell analysis to identify three white adipocyte populations characterized by unique expression profiles of three gene markers: Wilms tumor 1 (Wt1, type 1), transgelin (Tagln, type 2) and Myxovirus 1 (Mx1, type 3) [88]. In addition, clonal cell analysis and lineage tracing models revealed differences in metabolism and gene expression across these three populations, and that WAT depots are comprised of these 3 distinct adipocyte populations that differ in abundance [88].

1.2 Lipid Homeostasis

1.2.1 Lipid droplets

Lipid droplets consist of a core composed of triacylglycerols (TAGs) and cholesterol esters enveloped by a monophospholipid layer and are coated with various proteins including ATGL (adipose triglyceride lipase) [89]. Lipid droplets are mainly found in adipocytes, hepatocytes, mammary epithelial cells and steroidogenic cells [89]. Furthermore, the composition of the lipid core varies between cell types. Lipid droplets are not found only in mammals, but also in plants, bacteria and insects [90, 91]. Lipid droplets were initially thought of only having roles in lipid storage and preventing lipotoxicity; however, recent reports of the presence of proteins such as Rab GTPases on the lipid droplet surface suggest that they have additional roles in lipid trafficking and lipid metabolism [92]. Proteins found on the surface of lipid droplets include perilipin A (PLIN1), adipocyte differentiation-related protein (ADRP or PLIN2), and tail-interacting protein of 47 kDa (TIP47 or PLIN3), all of which contain a conserved sequence region called the PAT domain [93].

Whereas PLIN3 is highly expressed in all tissues, PLIN1 and PLIN2 are mostly expressed in WAT and liver respectively [94]. In adipocytes, perilipin A regulates lipid metabolism by controlling the access of lipases to the lipid droplets. Upon phosphorylation by protein kinase A, perilipin no longer blocks lipases found on the surface of lipid droplets from hydrolyzing TAGs stored in the lipid core. ADRP, which was named based on its early induction during adipocyte differentiation, has roles in the formation and stabilization of small lipid droplets [94] and is replaced with PLIN1 as preadipocytes mature. [95, 96]. Despite initially being implicated with intracellular trafficking of lysozymes, PLIN3 was reported to contribute towards lipid droplet stabilization [97].

1.2.2 Lipolysis

1.2.2.1 Key players in the lipolytic pathway

While white adipose tissues serve as sites for the storage of excess energy in the form of triglycerides, they also regulate the release and mobilization of stored triglycerides to other tissues that require energy in a process called lipolysis [98]. Lipolysis is a chemical pathway whereby triglycerides are sequentially hydrolyzed into FFAs and acylglycerols. Lipolysis is modulated by catecholamines, which bind either to β-adrenergic receptors to stimulate lipolysis or α2-adrenergic receptors to inhibit lipolysis [99]. In the case of lipolysis, binding of endogenous catecholamines such as norepinephrine to G-protein coupled β-adrenergic receptors (GPCRs) causes the α-subunit of heterotrimeric G-proteins to dissociate from the β and γ subunits. As a result, the Gα subunit stimulates the activity of adenylyl cyclase, increases production of the second messenger cAMP, activation of PKA, and the subsequent phosphorylation of HSL and transcription factors (Figure 3) [98]. Three enzymes are involved in the sequential hydrolysis of triglycerides to yield glycerol and FFA: adipose triglyceride lipase (ATGL), hormone sensitive lipase (HSL), and monoacylglycerol lipase (MAGL). ATGL catalyzes the hydrolysis of triacylglycerols (TAGs) into diacylglycerols (DAGs), which are subsequently hydrolyzed into monoacylglycerols (MAGs) by HSL. Lastly, MAGL hydrolyzes MAGs into free fatty acids and glycerol. A study that used ATGL-deficient mice and small-molecule inhibitors for HSL suggests that ATGL and HSL account for at least 90% of lipid hydrolysis in murine WAT [100].

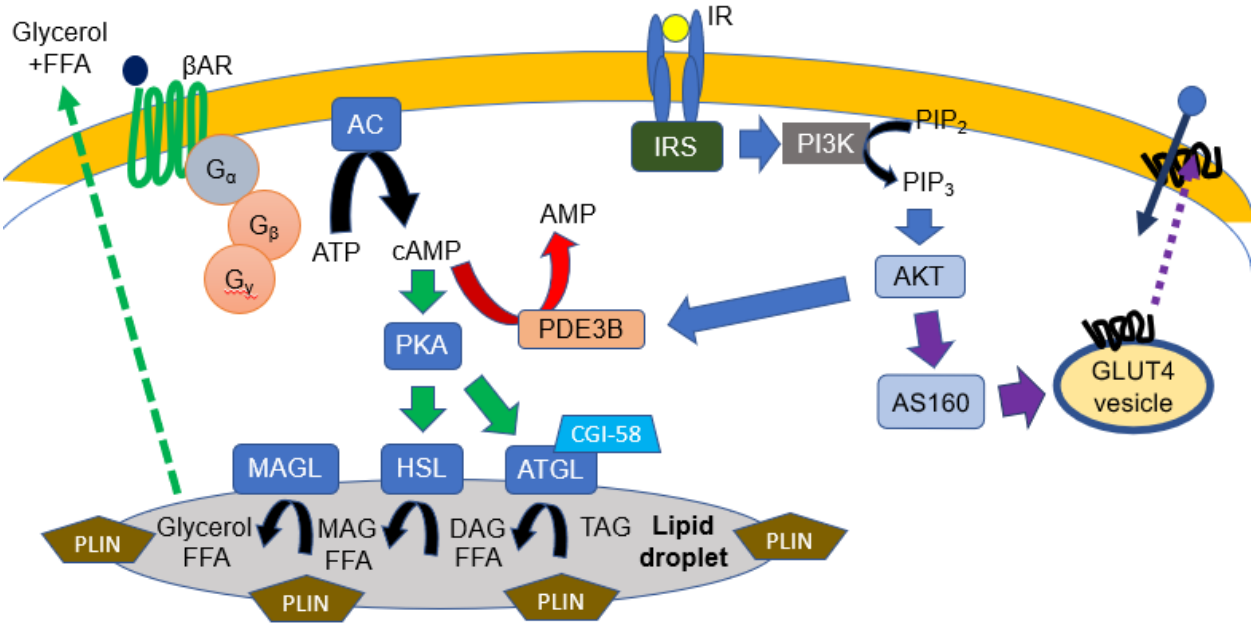

Figure 3: Lipolysis pathway in adipocytes. Stimulation of lipolysis involves catecholamines binding to β-adrenergic receptors and generation of the second messenger cAMP. Insulin signaling inhibits lipolysis through PI3K/AKT-mediated activation of PDE3B, which converts cAMP to AMP. AC, adenylyl cyclase; βAR, β-adrenergic receptor; CGI-58, comparative gene identification-58; HSL, hormone sensitive lipase; IR, insulin receptor; IRS, insulin receptor substrate; PDE3B, phosphodiesterase 3B; PIP_2, phosphatidylinositol 4,5-bisphosphate; PIP_3, phosphatidylinositol (3,4,5)-trisphosphate; PLIN, perilipin

1.2.2.2 HSL

Although HSL has been shown to exhibit broad specificity in hydrolyzing TAGs, DAGs, and MAGs, it was reported to have greater specificity for DAGs which are hydrolyzed approximately 10 times faster than TAGs [101, 102]. Several findings challenged the initial belief that HSL was the sole rate-limiting enzyme involved in the hydrolysis of TAGs. One example was the difference in the relative fold increase in β-adrenergic stimulated lipolysis from basal conditions (50-fold) compared to the fold increase in the specific activity of HSL (less than 2-fold) upon stimulation [102]. Furthermore, Haemmerle and colleagues observed that HSL knockout (HSL KO) mice only displayed a 30-40% reduction in FFA release compared to wild-type littermates. While these mice also displayed an accumulation of DAGs in adipose tissue, muscle, and testis, no TAG accumulation was observed in adipose or non-adipose tissue [103].

Taken together, these observations suggested that other lipases were involved in lipolysis (see sections 1.2.2.3 and 1.2.2.4).

Regulation of HSL activity is controlled by several factors. For instance, PKA has been shown to regulate HSL via phosphorylation at multiple sites including Ser650 in humans and Ser563, Ser659, and Ser660 in rat [104, 105]. Furthermore, β-adrenergic stimulation and insulin have opposing roles in modulating HSL activity, as the former condition strongly induces HSL activity and the latter inhibits its activity. Insulin inhibits lipolysis by activating AKT (also called PKB) and activates phosphodiesterase 3B which converts cAMP to 5'AMP (Figure 3) [106]. Under basal conditions, HSL resides in the cytoplasm and PLIN1 prevents HSL from accessing the lipid droplet. Upon stimulation of lipolysis, PKA phosphorylates multiple PLIN1 residues, including Ser81, Ser222, Ser272, Ser433, Ser492 and Ser517. As a result, PLIN1 interacts with and activates phosphorylated HSL which is found at the lipid droplet and is no longer restricted from hydrolyzing lipid droplets [107, 108]. Although PLIN1 was initially believed to be essential for HSL translocation, Miyoshi and colleagues demonstrated by cell fractionation and confocal microscopy that translocation of HSL to the lipid droplet surface was still possible in the presence of PLIN1 devoid of its six PKA-binding sites. This suggests that PLIN1 and PKA are not the sole proteins that mediate the activation of HSL.

1.2.2.3 ATGL

ATGL is also known as desnutrin and patatin-like phospholipase domain containing 2 (PNPLA2) and is highly selective for TAGs as it hydrolyzes them 10 times faster than DAGs [109]. Reports of significant reductions in TAG hydrolase activity following ATGL immunoprecipitation from human and mouse adipose tissue lysates suggested that ATGL may be responsible for hydrolyzing most TAGs [109, 110]. The contributions of ATGL in lipolysis and its role as the principal enzyme implicated in the

hydrolysis of TAGs were further substantiated by studies involving ATGL knockout (ATGL KO) mice. Haemmerle and colleagues observed that ATGL KO mice displayed significant reductions in TAG hydrolase activity, enlarged adipose tissues, and accumulated lipids in the heart causing cardiac dysfunction [111]. ATGL KO mice were also cold-sensitive as they reduced their body temperature and oxygen consumption when fasted. This was explained by the failure of WAT and BAT to mobilize adequate amounts of FFA which was evident from the nearly 70% decrease in isoproterenol-stimulated FFA release and significantly reduced plasma FFA levels in ATGL KO mice [111].

At least two serine residues have been identified as phosphorylation sites in murine ATGL: Ser406 and Ser430 [89]. Similarly, Bartz et al. identified Ser404 and Ser428 as phosphorylation sites in human ATGL [89]. Despite the identification of these phosphorylation sites, PKA was shown not to play a role in ATGL phosphorylation [109]. Ahmadian et al. demonstrated that ATGL phosphorylation was mediated by AMP-activated kinase (AMPK) at Ser406 and resulted in an increase in lipase activity [112]. However, a recent study from Pagnon et al. called into question whether phosphorylation of murine ATGL was strictly PKA-independent. Pagnon and colleagues showed that whereas both PKA and AMPK were able to phosphorylate Ser406 *in vitro*, only PKA could phosphorylate Ser406 *in vivo*. This was based on observations of pharmacological PKA inhibitors blocking the increase in β-adrenergic-stimulated phosphorylation at Ser406. Furthermore, no increases in AMPK activity in adipose tissue of fasted mice was observed, despite increases in phosphorylation of Ser406 [113]. Thus, this study called into question the previously established roles (or lack thereof) of AMPK and PKA in regulating lipolysis by phosphorylating mouse ATGL to modulate its activity.

Unlike HSL, ATGL requires a coactivator protein called comparative gene identification-58 (CGI-58) or α/β hydroxylase domain containing protein 5 (ABDH5) to achieve full TAG hydrolase activity. This was demonstrated in mouse models that reported up to a 20-fold increase in ATGL hydrolase activity in the presence of CGI-58 [114]. ATGL, which is found both in the cytoplasm and on the lipid droplet

surface, has also been reported to be indirectly regulated by perilipin. Studies point to perilipin regulating ATGL activity by controlling the accessibility of ATGL to its coactivator CGI-58 [115, 116]. In the basal state, perilipin binds to CGI-58 and prevents ATGL activation. In the stimulated state, PKA phosphorylates perilipin resulting in the dissociation of the perilipin – CGI58 complex. Consequently, CGI-58 is free to bind to and activate ATGL. Miyoshi and colleagues showed that PKA-mediated phosphorylation of perilipin at Ser517 was critical for ATGL activation as mutation of this site reduced forskolin-stimulated glycerol and FFA release by 95% in adipocytes derived from mouse embryonic fibroblasts [116].

1.2.2.4 MAGL

MAGL catalyzes the conversion of monoglycerides to glycerol and FFA. MAGL was previously reported to exhibit high specificity for MAGs [117]. Although MAGL is abundantly expressed in several tissues, the highest expression is seen in WAT. MAGL is found in the cytoplasm, plasma membrane and on the lipid droplet surface [118, 119]. In comparison to HSL and ATGL, very little is known about the regulation of MAGL [119]. In one study involving MAGL knockout mice, Taschler et al. reported a 35% reduction in stimulated lipolysis and MAG hydrolase activity [120]. This suggests that other recently discovered monoacylglycerol lipases including α/β hydrolase domain-containing protein 6 (ABHD6), ABDH12, and fatty acid amide hydrolase (FAAH) likely contribute to MAG hydrolysis. While the above-mentioned lipases were determined to display MAG hydrolase activity *in vitro*, the *in vivo* contributions and implications of these lipases to MAG hydrolysis remain to be elucidated. Lastly, interest in the contributions of MAGL outside of lipolysis stem from its reported role in degrading 2-arachidonylglycerol (2-AG), a signaling molecule belonging to the family of endogenous lipids known as endocannabinoids [121]. Endocannabinoids bind to G-protein coupled cannabinoid receptors to regulate energy homeostasis, lipid metabolism and food intake [122].

1.2.3 Lipogenesis

1.2.3.1 Overview of lipogenesis

De novo lipogenesis is a pathway whereby excess carbohydrates are used to synthesize free fatty acids, which are later converted into triglycerides for storage, particularly in white adipose tissue and the liver (Figure 4). Citrate produced from glucose undergoing glycolysis, pyruvate processing, and the tricarboxylic acid (TCA) cycle is shuttled from the mitochondria to the cytosol to generate acetyl-CoA by ATP-citrate lyase (ACLY). Fatty acids are then obtained from acetyl-CoA through a series of reactions catalyzed by the enzymes acetyl-CoA carboxylase (ACC1), fatty acid synthase (FASN), and stearoyl-CoA desaturase-1 (SCD-1). ACC1 and FASN are the two principle enzymes involved in the *de novo* lipogenesis pathway, as the former enzyme catalyzes the conversion of acetyl-CoA to malonyl-CoA and the latter enzyme converts malonyl-CoA into palmitate. The generation of palmitate, the first fatty acid product, is the rate-limiting step of the *de novo* lipogenesis pathway. Palmitate is elongated and saturated by enzymes including SCD-1 to generate various complex fatty acids, such as palmitoleic acid, steric acid, and oleic acid [123]. Regulation of these two principle enzymes are controlled by sterol-response-element-binding protein 1c (SREBP1c) and carbohydrate-response-element-binding protein (ChREBP). The roles of these transcription factors as the dominant regulators of *de novo* lipogenesis varies across different cell types, as SREBP1c is the main regulator in the liver and ChREBP is the main regulator in WAT [5].

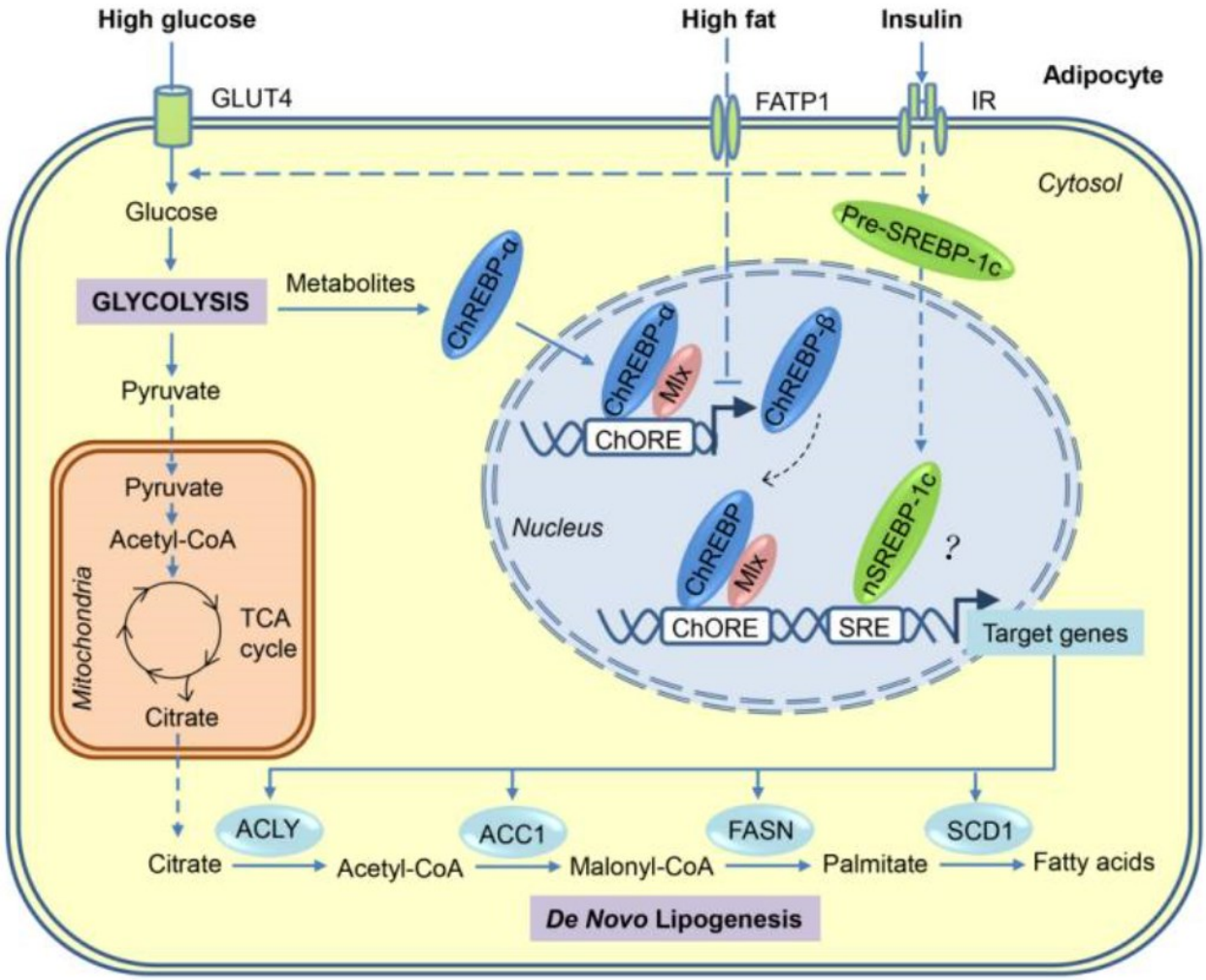

Figure 4: The *de novo* lipogenesis pathway in adipocytes. Glucose is metabolized into pyruvate through glycolysis and is later processed into acteyl-coA which enters the TCA cycle to generate citrate. The enzymes ACLY, ACC1, FASN, and SCD-1 catalyze a series of reactions to convert citrate into palmitate which undergoes additional processing to synthesize various fatty acids. The expression of these enzymes is regulated by the transcription factors ChREBP and SREBP-1c, which in turn are respectively stimulated by high glucose and insulin. ACLY, ATP citrate lyase; ACC1, Acetyl-CoA carboxylase 1; ChREBP, carbohydrate-response element binding protein; ChORE, carbohydrate response element; FASN, fatty acid synthase; SREBP-1c, Sterol-responsive element binding protein; SRE, sterol response element; SCD-1, stearoyl-CoA desaturase. Image taken from [123].

1.2.3.2 SREBP-1c

Sterol-responsive element binding proteins (SREBPs) are a class of transcription factors that possess the basic helix-loop-helix-leucine zipper (bHLH-Zip) domain for binding to DNA. The SREBP family is comprised of three isoforms: SREBP-1a, SREBP-1c, and SREBP-2. SREBP-1a activates genes involved in cholesterol, fatty acid, and triglyceride synthesis. SREBP-1c and SREBP-2 have more restrictive roles, as they respectively promote expression of genes related to fatty acid synthesis and cholesterol synthesis [124]. SREBPs are initially synthesized in their inactive form consisting of an amino-terminal domain containing the bHLH-Zip region, a hydrophobic transmembrane region, and a carboxy-terminal regulatory domain. When intracellular cholesterol levels are low, the escort protein and sterol sensor SREBP cleavage-activating protein (SCAP) binds and directs SREBP to the Golgi apparatus where it is proteolytically cleaved by two proteases, Site-1 and Site-2 protease (S1P and S2P). The activated amino-terminal domain translocates to the nucleus and binds to specific sterol response elements (SRE) in promoter regions of genes associated with fatty acid and cholesterol synthesis to drive their expression. Some target genes of SREBP-1c include ACLY, ACC1, FASN, and SCD-1 [124]. This process is also promoted by insulin. In hepatocytes, insulin also promotes transcription *of SREBP-1c* through the PI3K/AKT pathway that activates the downstream target mammalian target of rapamycin complex 1 (mTORC1) [125-127].

Loss of function and overexpression models for SREBP-1 have been utilized to examine its contributions to lipogenesis. Shimano and colleagues report that systemic deletion of SREBP-1 decreased hepatic lipogenesis but increased hepatic SREBP-2 levels and SREBP-2-mediated cholesterol synthesis. Interestingly, adiposity and lipogenic gene expression in WAT were not affected [128]. While adipocyte-specific SREBP knockout models have yet to be reported, adipocyte-specific SREBP overexpression studies have been conducted for the SREBP-1a and SREBP-1c isoforms. In a study by Horton et al., increased lipogenesis, hypertrophy, and fatty acid release in adipose tissue were observed

[129]. In the case of SREBP-1c, Shimomura et al. observed impaired adipocyte differentiation, reduced adiposity, glucose intolerance and impaired insulin sensitivity [130]. When taken together, the loss of function and gain of function models for SREBP-1 suggest that SREBP-1 plays a minor role in adipocyte *de novo* lipogenesis.

1.2.3.3 ChREBP

Carbohydrate-response element binding proteins (ChREBPs) are also transcription factors that have a bHLH/Zip motif. The N-terminus domain contains regions regulating its nuclear localization, whereas the C-terminus domain contains the bHLH/Zip motif required for DNA-binding [131, 132]. To date, two ChREBPs isoforms have been identified: ChREBP-α and ChREBP-β. ChREBP activity is dependent on glucose levels. During fasting periods when glucose levels are low, elevations in plasma glucagon and epinephrine stimulate the activation of PKA, which along with AMPK, phosphorylates ChREBP-α. Consequently, the transcriptional activity of ChREBP-α is inhibited, and it is retained in the cytosol. During feeding and in high glucose conditions, intermediates of glucose metabolism, such as xylulose-5-phosphate (Xu-5-P) and glucose-6-phosphate (G6P), accumulate and activate protein phosphatase 2A, which dephosphorylates ChREBP-α. As a result, ChREBP-α translocates to the nucleus and binds to carbohydrate response elements in the promoter regions of ChREBP-α target genes involved in glycolysis and fatty acid synthesis. These genes are the same previously mentioned targets of SREBP-1c. ChREBP-α also induces the transcription of ChREBP-β, which upon feed-forward stimulation of its own expression activates its respective set of gene targets (Figure 4) [133-135].

Global knockout of ChREBP in mice led to decreases in adiposity, increased glucose tolerance, and reduced insulin sensitivity [136]. However, adipocyte-specific deletion of ChREBP was reported to decrease sucrose-induced lipogenesis only in liver while also impairing glucose tolerance and insulin sensitivity [137]. Conversely, Nuotio-Antar et al. reported that mice overexpressing ChREBP in adipose

tissue displayed a lean phenotype while lipogenesis in adipose tissue increased. Other metabolic phenotypes included improved glucose tolerance and insulin sensitivity [138]. The reports of increased adipocyte *de novo* lipogenesis in the adipocyte-specific overexpression model for ChREBP but not SREBP-1c suggests that between the two transcription factors, ChREBP is the principal activator of *de novo* lipogenesis in adipocytes.

1.2.3.4 ACC1

ACC1 catalyzes the carboxylation of acetyl CoA to produce malonyl CoA. In eukaryotes, ACC1 exists as a single multifunctional polypeptide that containing domains of a biotin carboxyl carrier protein, a biotin carboxylase, and a transcarboxylase. Each monomer is approximately 265 kDa. In contrast, these three domains correspond to three separate proteins in prokaryotes [139]. ACC1 expression is transcriptionally regulated by SREBP-1c and ChREBP as previously described (Figure 4). In addition, ACC1 activity is modulated post-translationally by AMPK-mediated phosphorylation. Activation of AMPK by glucagon and epinephrine results in the phosphorylation and inactivation of ACC1, whereas insulin-mediated activation of protein phosphatase 2A reverses this and activates ACC1. In addition, citrate, an upstream precursor in the *de novo* lipogenesis pathway, allosterically binds and partially activates ACC1 [123]. The important role of ACC1 in *de novo* lipogenesis was demonstrated by Mao et al. who reported that liver-specific ACC1 mice displayed reduced hepatic lipid content compared to control mice placed on a fat-free diet [140]. However, this protective reduction in hepatic lipid content was lost when the liver-specific knockout mice were put on high-fat diet.

1.2.3.5 FASN

FASN catalyzes the synthesis of palmitate from malonyl CoA and exists in two forms: FASN I (type 1) and FASN II (type 2). FASN I is found in animals and fungi and exists as a multifunctional homodimeric polypeptide [141, 142]. In plants and bacteria, FASN II exists as a series of individual

monofunctional enzymes whose domains are homologous to FASN I orthologs [143]. FASN is transcriptionally regulated by the previously mentioned transcription factors SREBP-1c and ChREBP (Figure 4). Mouse models have identified key roles of FASN in lipid synthesis and cellular signaling. In one study, liver-specific FASN knockout mice that were fed a zero-fat diet displayed exacerbated hepatic steatosis [144]. This suggests that the protection against steatosis observed in ACC1 knockout mice fed a fat-free diet is likely attributed to the reduction in malonyl-CoA production [145]. In another report by Lodhi et al, adipocyte-specific FASN knockout mice had a lean phenotype resulting from impaired PPARγ activation, and displayed increased energy expenditure and beiging of subcutaneous adipose tissue. activation. These mice were also protected from diet-induced obesity. In addition, decreased transcriptional PPARγ activity and adipogenesis was shown to result from a reduction in the synthesis of PPARγ agonists such as specific alkyl ether lipids [146].

1.3 14-3-3 proteins

1.3.1 Structure

Since their original discovery in bovine brain homogenates over 50 years ago, a renewed interest has been taken in understanding the roles of molecular scaffolds belonging to the 14-3-3 protein family. The name 14-3-3 is derived from their discovery in the 14th fraction of DEAE-cellulose chromatography and migration position 3.3 following gel electrophoresis [147]. 14-3-3 proteins are 28-33 kDa acidic proteins. In mammals, seven isoforms comprise the 14-3-3 protein family: β, γ, ε, η, σ, θ and ζ. Although these isoforms are highly conserved, their individual expression profiles vary between tissues and cell types [148]. 14-3-3 proteins often dimerize to form either homodimers or heterodimers in order to interact with client proteins [149, 150]. Each monomer consists of nine α-helices that are arranged in an antiparallel manner. Furthermore, a monomer consists of the N-terminus, a conserved core region, and the C-terminus. Although both the N-terminus and C-terminus display variability across the isoforms, only the N-terminus contains the residues required for dimerization [151, 152]. In the core region, four

α-helices, helices 3, 5, 7, and 9 arrange themselves in such a way that an amphipathic groove is formed, whereby one side has a cluster of polar residues and the other side has a cluster of non-polar residues [151]. This amphipathic groove comprises the ligand binding domain that allows the 14-3-3 proteins to interact with their target proteins. Two classical types of phosphorylation-dependent and high-affinity 14-3-3 binding motifs were identified: RSX pS/T XP (mode 1) and RXXX pS/T XP (mode 2) where pS/T and X represent phosphorylated serine or threonine and any amino acid respectively [153]. 14-3-3 proteins are also capable of binding to non-phosphorylated client proteins. Dimerization also allows 14-3-3 proteins to simultaneously bind to two targets [154]. These phospho-motifs are generated by kinases, such as PKA, AKT and PKC [147, 153]. Upon binding, 14-3-3 proteins can spatially and temporally control the localization of their binding partners, regulate the activity of their targets, and mediate protein interactions that involve the client protein [151, 152, 155].

1.3.2 Function

14-3-3 proteins are also called tyrosine and tryptophan hydroxylase activators (YWHAs). This alternative name comes from the discovery of their first reported function, which was the regulation of tyrosine and tryptophan hydroxylases [156]. Tyrosine and tryptophan hydroxylases catalyze the rate-limiting steps of catecholamine and serotonin synthesis, respectively. 14-3-3 proteins are often referred as molecular scaffolds due to their ability to interact with one or several target proteins implicated in a signaling pathway. For example, 14-3-3β and 14-3-3θ were reported to facilitate interactions between PKC and RAF-1 in the RAF/MEK/ERK cascade that regulates cell fate [157]. Various roles have been reported for 14-3-3 proteins with respect to cellular and organismal metabolism and include the regulation of the cardiac isoform phosphofructo-2-kinase/fructose-2,6-biphosphatase (PFK-2) [158, 159] and glyceraldehyde-3-phosphate dehydrogenase (GAPDH) involved in gluconeogenesis and glycolysis [160-162]. Other 14-3-3 targets that have been cited include cell division cycle 25B (CDC25B) involved in progression of the cell cycle [163-165] and Bcl-2-associated death promoter (BAD) involved in apoptosis

and insulin secretion by pancreatic β-cells [166, 167]. Lim et al. previously reported on the metabolic contributions of the zeta isoform with respect to glucose homeostasis using a systemic knockout mouse model. They observed that 14-3-3ζ knockout mice had improved oral glucose tolerance despite displaying insulin resistance. This was attributed to elevated levels of GLP-1 [168].

1.3.3 Implication of 14-3-3 proteins on adipocyte development

We previously demonstrated that 14-3-3ζ has essential roles in adipogenesis using a combination of *in vitro* and *in vivo* models. We reported that only 14-3-3ζ was required for the differentiation of 3T3-L1 pre-adipocytes [169], and that 14-3-3ζ affects alternative splicing of *Pparg* mRNA during adipocyte differentiation [170]. We also reported that systemic 14-3-3ζ knockout (14-3-3ζKO) mice displayed significant reductions of fat specifically in visceral depots and had smaller gonadal adipocytes compared to wild-type littermates. [169]. Furthermore, transgenic mice overexpressing 14-3-3ζ gained more weight and fat mass compared to wild-type mice fed a high-fat diet (HFD). Metabolic phenotype studies revealed that 14-3-3ζ overexpression did not impair glucose tolerance or insulin sensitivity [169]. Regarding the insulin-mediated glucose uptake pathway that is dependent on GLUT4 in adipocytes, 14-3-3ζ was shown to interact with several targets including IRS1, IRS2, and AS160 [171, 172].

1.4 Hypothesis and objectives

We demonstrated in a previous report that 14-3-3ζ has essential roles in the development of adipocytes and adipose tissue [169, 170]. However, the contributions of 14-3-3ζ to the function of mature adipocytes are still not known. Furthermore, conclusions regarding the contributions of 14-3-3ζ to adipogenesis were based in part on mice models where 14-3-3ζ was either systemically deleted or systemically overexpressed. A limitation in using these models is that they do not allow for contributions of 14-3-3ζ specifically in adipocytes to be evaluated. This master's project was pursued to address these outstanding issues.

Our hypothesis was that decreasing 14-3-3ζ expression in adipocytes will impair the function of mature adipocytes. In order to test this hypothesis, the first objective of this project is to obtain a clearer understanding of how 14-3-3ζ contributes to adipocyte-specific processes. We begin this endeavor by determining if 14-3-3ζ plays a role in lipolysis, as 14-3-3 protein binding motifs have been identified in ATGL and HSL [173]. This suggests that 14-3-3ζ may have regulatory roles in lipolysis. The second objective of this project is to assess whether the deletion of 14-3-3ζ specifically in adipocytes affects whole-body metabolism. This determination requires the metabolic characterization of adipocyte-specific 14-3-3ζ knockout mice (adi14-3-3ζKO) that will be used in this project.

2.0 Research Article

14-3-3zeta is required for PKA-dependent lipolysis in mature adipocytes

Abel Oppong[1], Kadidia Diallo[1], Yves Mugabo[1], Gareth Lim[1]

[1] Department of Medicine, Université de Montréal and Centre de recherche du Centre hospitalier de l'Université de Montréal (CRCHUM), 900 Saint-Denis St., Montreal, QC, Canada H2X 0A9

Contributions of:

AO: Performed experiments, analyzed data, and wrote the manuscript
KD: Performed adipocyte morphological measurements (not included in memoire)
YM: Assisted with *in vivo* experiments and technical assistance with TAG measurements
GEL: Designed the study, analyzed data, and edited the manuscript. GEL is the guarantor of this work.

Corresponding author:

Gareth Lim, Ph.D.
Centre de recherche du Centre hospitalier de l'Université de Montréal (CRCHUM)
900 Saint-Denis St., Montreal, QC, Canada H2X 0A9
Telephone: (514) 890-8000 Extension 12927
E-mail: gareth.lim@umontreal.ca

Disclosure Statement: The authors have nothing to disclose

This paper is in preparation and will be submitted to the *Journal of Lipid Research* in 2 months.

2.1 Abstract

The molecular scaffold, 14-3-3ζ, was previously reported to have roles in the development of adipocytes. However, the contributions of 14-3-3ζ to processes such as lipolysis in mature adipocytes have yet to be elucidated. Herein, we demonstrate that 14-3-3ζ is necessary for lipolysis, as adipocyte-specific 14-3-3ζ knockout (adi14-3-3ζKO) mice and adipose tissue lacking 14-3-3ζ display impaired glycerol and FFA release following activation of the β3-adrenergic signaling pathway. Furthermore, HSL activation in gonadal adipose depots was decreased in adi14-3-3ζKO mice. These findings were recapitulated in siRNA-transfected 3T3-L1 adipocytes that exhibited reductions in phosphorylated and total forms of PKA substrates including HSL and CREB. 3T3-L1 adipocytes depleted of 14-3-3ζ also displayed reductions in lipase mRNA and impaired lipolysis in response to multiple agonists including isoproterenol, forskolin and dbcAMP. *In vitro* mechanistic studies point to 14-3-3ζ regulating lipolysis in a PKA-dependent manner. In addition, 14-3-3ζ appears to have roles in determining adipocyte maturity as mature adipocyte features including *Pparg* mRNA and PPARγ expression and triacylglycerol content are reduced in adi14-3-3ζKO adipose depots and 14-3-3ζ-depleted 3T3-L1 adipocytes. Collectively, these findings reveal a novel role for 14-3-3ζ in regulating PKA-dependent lipolysis.

2.2 Introduction

The primary function of white adipose tissue is the regulation of energy homeostasis. White adipocytes specialize in both the storage of triacylglycerols (TAGs) and the mobilization of free fatty acids (FFAs) to peripheral tissues to accommodate increases in metabolic demand that occur during exercise and fasting [98]. In WAT, FFAs are generated by the hydrolysis of TAGs in a process known as lipolysis. Stimulation of the lipolytic pathway involves the binding of catecholamines to β-adrenergic receptors and the subsequent generation of the second messenger cyclic adenosine monophosphate (cAMP), which activates protein kinase A (PKA) [98]. TAG hydrolysis is mediated by three lipases: adipose triacylglycerol lipase (ATGL), hormone sensitive lipase (HSL), and monoacylglycerol lipase (MAGL). These lipases, respectively, catalyze the sequential conversion of TAGs into diacylglycerols (DAGs), monoacylglycerols (MAGs), and finally FFAs and glycerol. One of these lipases, HSL, has been shown to be directly phosphorylated by PKA [104, 105].

The 14-3-3 family of molecular scaffolds are implicated in several cellular processes, such as proliferation, apoptosis and metabolism [169, 174, 175]. This stems from their ability to interact with target proteins via phosphorylated serine and threonine motifs to regulate their localization, activity and interactions with other proteins [153, 154]. We have previously reported that only one of these seven mammalian isoforms, 14-3-3ζ, was required for adipogenesis [169]. However, the role of 14-3-3ζ in mature adipocyte function has not been examined. To that end, our focus turned to understanding the contributions of 14-3-3ζ to adipocyte-specific processes, such as lipolysis. The identification of the 14-3-3ζ binding motifs on ATGL and HSL suggests that 14-3-3ζ may have a regulatory role in lipolysis [173].

Herein, we report that 14-3-3ζ is an important regulator of lipolysis, as adipocyte-specific 14-3-3ζ knockout (adi14-3-3ζKO) mice display impaired glycerol release and HSL activation. These observations are replicated *in vitro* with 3T3-L1 adipocytes transfected with siRNA directed against 14-3-3ζ. We also report on an unexpected role of 14-3-3ζ in the regulation of adipocyte maturity based on reduced mRNA levels for genes involved in adipogenesis, lipogenesis, fatty acid transport, and lipid content.

2.3 Materials and Methods

Animal husbandry

Adipoq-CreERT2^{Soff} mice (stock no. 025124) were purchased from the Jackson Laboratory. Cryopreserved sperm for *Ywhaz*-floxed (*Ywhaz*$^{fl/fl}$) mice were purchased from the International Mouse Phenotyping Consortium and rederived onto a C57BL/6J (CRCHUM Transgenesis Core) background. Sperm was derived from the breeding of mice with a knock-out first allele with FRT flippase-expressing mice (Ywhaz$^{tm1a(EUCOMM)Hmgu}$); https://www.mousephenotype.org/data/genes/MGI:109484). *Adipoq-CreERT2* and *Ywhaz*-floxed mice were maintained on a C57/BL6J background. Cre-LoxP technology was used to delete exon 4 of *Ywhaz* which encodes 14-3-3ζ, following intraperitoneal administration of tamoxifen (50 mg/kg b.w; Sigma Aldrich, St. Louis, MO) for five days at two months of age. Transgenic mice overexpressing 14-3-3ζ (TAP) on a CD1 background were provided by the laboratory of Dr. Amparo Acker-Palmer [169, 176]. All mice were maintained on a standard chow diet (Teklad diet no. TD2918) under 12-hour light/12-hour dark cycles in an environmentally controlled setting (22°C ± 1°C) with free access to food and water. All procedures were approved and performed in accordance with CIPA (Comité institutionnel de protection des animaux du CRCHUM) guidelines at the Université de Montréal Hospital Research Centre.

Cell Culture and transient transfections

3T3-L1 cells were maintained in DMEM (Life Technologies Corporation, Grand Island, NY), supplemented with 10% newborn calf serum (NBCS) and 1% penicillin/streptomycin (P/S) and were seeded onto 12-well plates (100,000 cells/well) or 10cm dishes (2x10^6 cells/dish) 2 days prior to the induction of differentiation. Confluent cells were treated with a differentiation cocktail (DMEM supplemented with 10% FBS, 1% P/S, 500 µM IBMX, 500 nM dexamethasone and 172 nM insulin) for 48 hours, followed by media replacement (DMEM with 10% FBS, 1% P/S and 172 nM insulin) every 2 days

for 7-8 days. Knockdown and overexpression of 14-3-3ζ was achieved by transfecting day 7-8 differentiated cells with scrambled control siRNA, 14-3-3ζ-specific siRNA (Ambion, Austin, TX), GFP control plasmids, or plasmids encoding 14-3-3ζ (14-3-3ζ IRES-GFP) using the Amaxa Cell Line Nucleofector Kit L, as per manufacturer's instructions (Lonza, Koln, Germany).

Metabolic phenotyping

For glucose tolerance tests, adi14-3-3ζKO mice were fasted for six hours and challenged with d-glucose (2 g/kg b.w.; VWR, Solon, OH) by intraperitoneal administration [168, 169]. For insulin tolerance tests, adi14-3-3ζKO mice were fasted for four hours and were injected intraperitoneally with Humulin R insulin (0.5 U/kg b.w; Eli Lilly, Toronto, ON) [168, 169]. Blood glucose was measured from tail blood with a Contour Next EZ glucose meter (Ascencia Diabetes Care, Basel, Switzerland).

Measurements of lipolysis

Adi14-3-3ζKO mice were injected with 1 mg/kg CL-316,243, a β3 adrenergic agonist (Sigma-Aldrich, St. Louis, MO) following an overnight fast [177]. TAP mice were injected with 10 mg/kg isoproterenol (Sigma-Aldrich), following an overnight fast. Blood was collected from the tail vein before and 30 minutes after receiving injections and was centrifuged at 13,000 RPM for 10 minutes to measure plasma glycerol and free fatty acids levels in both mice. To measure lipolysis *ex vivo,* gonadal adipose tissue was harvested and immediately placed into pH 7.4-adjusted Krebs-Ringer buffer (135 mM NaCl, 3.6 mM KCl, 0.5 mM NaH_2PO_4, 0.5 mM $MgCl_2$, and 1.5 mM $CaCl_2$) supplemented with 10 mM HEPES, 2 mM $NaHCO_3$, 5 mM glucose and 2% bovine serum albumin (BSA). Gonadal explants were treated with or without 1 µM isoproterenol (Sigma Aldrich) for two hours [177]. The supernatant was collected and centrifuged for 15 minutes at 1500 RPM. To measure lipolysis from differentiated 3T3-L1 cells (Zenbio, Research Triangle Park, NC), cells were incubated in starvation media consisting of pH 7.4-adjusted Krebs-Ringer buffer, 5 mM glucose and 0.2% BSA for two hours. Cells were then incubated in

experimental media consisting of pH 7.4-adjusted Krebs-Ringer buffer, 5 mM glucose and 2% BSA for two hours while treated with 1 µM isoproterenol (Sigma-Aldrich), 10 µM forskolin with 0.5 mM IBMX (Sigma-Aldrich), or 1 mM dibutyryl cAMP (Sigma-Aldrich). Supernatant was collected, and glycerol and free fatty acid (FFA) release was measured using triglyceride (Sigma-Aldrich) and non-esterified fatty acid (NEFA; Wako Diagnostics, Osaka, Japan) kits following the manufacturer's protocol.

RNA isolation and qPCR

After 48 hours, total RNA was isolated from differentiated 3T3-L1 cells using the RNeasy kit (Qiagen, Hilden, Germany). cDNA was generated using the High-Capacity cDNA Reverse Transcription kit (ThermoFisher Scientific, Vilnius, Lithuania). mRNA expression was measured by real-time qPCR with SYBR green chemistry using the QuantStudio 6-flex Real-time PCR System (Thermofisher Scientific) and *Hprt* as the housekeeping gene. No specific qPCR protocols were used. Primer sequences are listed in Supplementary Table 1.

Measurement of intracellular cAMP levels

Day 7 differentiated 3T3-L1 adipocytes were transfected with scrambled siRNA or siRNA targeting 14-3-3ζ. After 48 hours, cells were incubated in starvation media (pH 7.4-adjusted Krebs-Ringer buffer, 5 mM glucose, and 0.2% BSA) for two hours, followed by incubation in experimental media in the presence of 1 µM Iso or 20 µM forskolin with 0.5 mM IBMX for one hour. Lysates were harvested and intracellular cAMP levels were assayed using the cAMP Parameter Assay Kit (R&D Systems, Minneapolis, MN).

Immunoblotting and detection

Differentiated 3T3-L1 cells were lysed in RIPA buffer (0.9% NaCl, 1% v/v triton X-100, 0.5% sodium deoxycholate, 0.1% SDS, and 0.6% tris base) supplemented with protease and phosphatase inhibitors (Sigma-Aldrich) 48 hours after transfection. Proteins were resolved by SDS-PAGE on 10-12.5% gels for 1.5 – 2 hours and transferred to PVDF membranes using the Trans-blot turbo transfer system (Bio-Rad Laboratories, Hercules, CA). Antibodies and their concentrations are listed in Supplementary Table 2.

Oil Red-O (ORO) staining

Differentiated 3T3-L1 cells were stained with ORO (VWR). Cells were washed in PBS and incubated in ORO solution for 15 minutes. ORO incorporation was measured, as previously described [169].

Statistical Analyses

Data are expressed as mean ± standard error of the mean. Statistical analyses were performed using two-tailed Student' t-test or two-way ANOVAs with appropriate *post-hoc* tests. A p-value less than 0.05 was considered statistically significant.

2.4 Results

Adipocyte-specific deletion of 14-3-3ζ impairs lipolysis in mice

To investigate the contributions of 14-3-3ζ to mature adipocyte function, tamoxifen-inducible adipocyte-specific 14-3-3ζ knockout (adi14-3-3ζKO) mice were generated by deleting exon 4 of *Ywhaz* using Cre-LoxP technology. We first sought to validate our model and confirmed by qPCR that 14-3-3ζ expression was decreased in the gonadal white (gWAT), inguinal white (iWAT), and brown adipose (BAT) depots of male and female adi14-3-3ζKO mice following tamoxifen injection (Figures 1A and 1B). We also confirmed that 14-3-3ζ deletion did not alter transcript levels of the other 14-3-3 isoforms (Figure S1). We next conducted metabolic phenotype studies on the adi14-3-3ζKO mice. No differences in body weights between adi14-3-3ζKO and Cre+ wild-type littermate controls were observed (Figures 1C and 1D). Furthermore, adipocyte-specific deletion of 14-3-3ζ did not affect glucose metabolism as shown by intraperitoneal glucose tolerance test (IPGTT) and intraperitoneal insulin tolerance test (ITT) (Figures 1E-H).

We then focused on whether 14-3-3ζ can influence lipolysis. To achieve this, adi14-3-3ζKO mice were fasted overnight and challenged with CL-316,243, a β3-adrenergic agonist. Male adi14-3-3ζKO mice displayed a significant reduction in plasma glycerol levels following intraperitoneal administration of CL-316,243 (Figure 2A). Plasma glycerol levels were also lower in female adi14-3-3ζKO mice, although the difference was not significant (Figure 2B). In contrast, plasma FFA levels in male and female adi14-3-3ζKO mice were comparable to littermate controls following stimulation with CL-316,243 (Figures 2C and 2D). Our observation of impaired glycerol release in adi14-3-3ζKO mice prompted us to further examine the effect of 14-3-3ζ deletion on adipocyte function. To that end, male gWAT depots were harvested and stimulated with isoproterenol. Significant impairments in isoproterenol-mediated glycerol and FFA release were detected in adi14-3-3ζKO gonadal explants (Figures 2E and 2F).

HSL activation is impaired in adi14-3-3ζKO mice

As a first step to understanding the functional roles of 14-3-3ζ in lipolysis, we looked at lipase expression in the gWAT and iWAT of adi14-3-3ζKO mice. A significant reduction in *Atgl* mRNA was observed in the gWAT of male knockout mice (Figure 3A). Interestingly, mRNA levels of *Pparg* also decreased following deletion of 14-3-3ζ in adipocytes (Figures 3E and 3F). Immunoblotting was next performed to determine whether 14-3-3ζ deletion altered lipase expression at the protein level. ATGL levels remained unchanged between the gWAT of male adi14-3-3ζKO and Cre+ wild-type mice (Figure 3G). However, adi14-3-3ζKO mice displayed noticeable reductions in both the phosphorylated and total levels of HSL. Furthermore, reductions in the PPARγ2 isoform, which is specifically expressed in adipocytes [178], were observed in the gWAT of male adi14-3-3ζKO mice (Figure 3H). This is consistent with qPCR results that suggest downregulation of *Pparg* mRNA expression following adipocyte-specific ablation of 14-3-3ζ (Figure 3E).

14-3-3ζ depletion decreases lipolysis in 3T3-L1 cells in a PKA-dependent manner

To further elucidate the regulatory role of 14-3-3ζ in lipolysis, differentiated 3T3-L1 adipocytes were transfected with siRNA against 14-3-3ζ to examine the impact on the lipolytic pathway. As shown in Figure 4A, treatment with various concentrations of siRNA resulted in more than a 90% reduction in *Ywhaz* levels compared to cells transfected with a scrambled, control siRNA. qPCR results confirmed that siRNA-mediated knockdown of 14-3-3ζ did not affect mRNA levels of the six other 14-3-3 isoforms (Figure S2). Immunoblotting was also performed to validate 14-3-3ζ knockdown occurring at the protein level following RNA silencing of *Ywhaz* (Figure 4B). Next, glycerol and FFA levels were measured in the supernatant of 14-3-3ζ-depleted 3T3-L1 adipocytes treated with different agonists that stimulate lipolysis. These agonists included isoproterenol, forskolin, and dibutyryl cAMP (dbcAMP). Knockdown of

14-3-3ζ led to significant reductions in both glycerol and FFA release compared to control cells for all agonists (Figures 4C and 4D).

Our focus next turned to determining where 14-3-3ζ acts in the lipolytic pathway to exert its regulatory role. We first looked at message expression of the adrenergic β-receptor isoforms (*Adrb1, Adrb2,* and *Adrb3*) in 14-3-3ζ-depleted adipocytes. While there was no change in mRNA levels for *Adrb1* and *Adrb2*, a significant reduction in mRNA levels of *Adrb3,* which is mainly expressed in adipocytes [179], was observed (Figure 4E). To examine whether impaired lipolysis resulting from 14-3-3ζ depletion was attributed to altered cAMP degradation or production, we next measured transcript levels of various phosphodiesterase isoforms in siRNA-transfected 3T3-L1 adipocytes, and no significant differences were observed in any of the isoforms examined (Figure 4F). To evaluate whether adenylyl cyclase activity was affected by 14-3-3ζ depletion, intracellular cAMP levels were measured in 3T3-L1 lysates treated with isoproterenol, and no differences were observed (Figure 4G). We next looked at lipase expression and observed significant reductions in *Atgl* and *Hsl* mRNA transcripts in 14-3-3ζ-depleted cells (Figure 4H). The effect of 14-3-3ζ knockdown on lipase expression was evaluated by immunoblotting, which revealed that phosphorylated and total HSL levels were reduced in siRNA-transfected 3T3-L1 cells (Figure 4I). This is in agreement with the adi14-3-3ζKO model that demonstrated decreased HSL activation and total expression following 14-3-3ζ deletion in adipocytes (Figure 3H). Immunoblotting for CREB, a transcription factor and phosphorylation target of protein kinase A, revealed similar reductions in phosphorylated and total forms of CREB (Figure 4I).

Overexpression of 14-3-3ζ potentiates lipolysis *in vitro*

The effect of 14-3-3ζ overexpression on lipolysis was also explored using both *in vitro* and *in vivo* models. Plasmids encoding 14-3-3ζ, or GFP as a control were introduced into differentiated 3T3-L1 adipocytes by electroporation, and 14-3-3ζ overexpression was confirmed by immunoblotting (Figure

S3A). FFA release was significantly potentiated in 3T3-L1 cells overexpressing 14-3-3ζ (Figure S3B). In contrast, TAP mice overexpressing 14-3-3ζ did not display a potentiated lipolytic response to isoproterenol (Figures S3C-F).

14-3-3ζ is required for maintaining the mature adipocyte phenotype

Our observation of decreased *Pparg* mRNA expression in gWAT of adi14-3-3ζKO mice (Figures 3E and 3F) prompted us to evaluate whether adipocyte maturity was altered in 14-3-3ζ-defficient 3T3-L1 adipocytes. qPCR revealed significant reductions in transcript levels for adipocyte markers including *Pparg, Fabp4, Fasn, and Lpl* in 14-3-3ζ-depleted 3T3-L1 adipocytes. (Figure 5A). Given that one of the main functions of white adipose tissue is energy storage and mobilization, we looked at whether 14-3-3ζ depletion altered triglyceride content levels in 3T3-L1 adipocytes. A significant reduction in TAG levels was observed in 14-3-3ζ-depleted lysates (Figure 5B). This was recapitulated using Oil Red-O, which demonstrated a significant reduction in intensity (Figure 5C). Moreover, marked reductions in lipid droplets were observed in 14-3-3ζ-depleted cells (Figure 5D).

2.5 Discussion

The aim of this study was to examine the contributions of 14-3-3ζ to the function of mature adipocytes. As 14-3-3ζ has been shown to regulate activities of proteins implicated in diverse metabolic processes [159, 160, 167, 172, 180-182], we hypothesized that 14-3-3ζ had essential roles in adipocyte-specific processes, such as lipolysis. Mice with targeted deletion of 14-3-3ζ specifically in adipocytes displayed impaired lipolysis, as well as reduced *Atgl* mRNA expression and HSL activation. These findings were recapitulated in 3T3-L1 cells depleted of 14-3-3ζ by siRNA. Mechanistic studies done in 3T3-L1 cells suggest that 14-3-3ζ regulates lipolysis in a PKA-dependent manner to modulate lipase expression and activation (Figure 6). In addition, decreased *Pparg* mRNA and PPARγ expression was observed in both *in vivo* and *in vitro* 14-3-3ζ models, suggesting that 14-3-3ζ plays an additional role in determining adipocyte maturity. Despite these observations, adipocyte specific deletion of 14-3-3ζ did not produce any changes in body weight. Furthermore, systemic overexpression of 14-3-3ζ did not affect lipolysis in mice.

Adi14-3-3ζKO mice were used to investigate the contributions made by 14-3-3ζ specifically in adipocytes. Male adi14-3-3ζKO mice displayed significantly lower plasma glycerol levels following intraperitoneal injections of the β3-adrenergic agonist CL-316,243, and this observation was recapitulated *ex vivo,* as gonadal WAT explants from adi14-3-3ζKO mice displayed significant reductions in glycerol and FFA release when stimulated with isoproterenol. Although 14-3-3-binding sites have been previously reported for ATGL and HSL, thus implicating roles of 14-3-3 proteins [112, 173], our results demonstrate for the first time that 14-3-3ζ directly regulates lipolysis in adipocytes possibly through modulating HSL activation. To our knowledge, no prior studies regarding the contribution of 14-3-3 proteins to lipolysis have been reported. This study expands on our knowledge about the roles of 14-3-3 proteins in lipid metabolism, which was previously limited to fatty acid synthesis. Affinity proteomics identified fatty acid synthase as a binding partner of 14-3-3 proteins [180, 182], but the

significance of this interaction was not further explored. In addition, 14-3-3 proteins were shown to interact with ChREBP, a key transcription factor that regulates *de novo* lipogenesis, and prevent its translocation from the cytosol to the nucleus [124, 131, 132]. Future studies are required to further understand how 14-3-3 proteins, and specifically 14-3-3ζ, regulate the activity of enzymes involved in lipolysis and lipogenesis.

3T3-L1 cells are a favoured model for adipocyte biology, as they recapitulate many aspects of primary mouse adipocytes such as signaling pathways involved in lipolysis and adipogenesis [183, 184]. Our investigation of the *in vitro* contributions of 14-3-3ζ to lipolysis began with treating 14-3-3ζ-depleted 3T3-L1 adipocytes with isoproterenol, forskolin, and dbcAMP, which activate the β-adrenergic receptor, adenylyl cyclase, and PKA, respectively. With all agonists, significantly impaired glycerol and FFA release were observed following 14-3-3ζ depletion. These results agree with the *in vivo* and *ex vivo* lipolysis data that suggest impaired adipocyte function. Intracellular cAMP levels were comparable between control and 14-3-3ζ-depleted 3T3-L1 lysates suggesting that 14-3-3ζ does not affect cAMP generation by adenylyl cyclase. Thus, regulation of lipolysis by 14-3-3ζ likely occurs downstream of cAMP generation with PKA being a possible target. This is consistent the finding that 14-3-3 proteins bind to and regulate the activity of PKA during growth cone turning responses in neurons [185]. Coimmunoprecipitation studies done by Kent et al. reported that the gamma and epsilon 14-3-3 isoforms bind to the RIIα and RIIβ regulatory subunits of PKA and could modulate PKA activity [185]. Further studies are required to examine if 14-3-3ζ has similar roles in PKA binding and the regulation of its activity. It is also possible that 14-3-3ζ influences lipolysis by facilitating interactions between PKA and its substrates including HSL and CREB. Indeed, 14-3-3 proteins were reported to act as molecular adapters to promote interactions between PKC and the PKC substrate RAF-1 [157]. Coimmunoprecipitation studies revealed that binding of 14-3-3ζ to the PKC regulatory domain was required to form a PKC-14-3-3ζ-RAF-1 ternary complex that was mediated by 14-3-3β and 14-3-3θ [157].

In the current study, reductions in *Pparg* mRNA and protein expression were observed in 14-3-3ζ-depleted 3T3-L1 cells and in the gWAT and iWAT of adi14-3-3ζKO mice. This suggests a loss in adipocyte maturity whereby some adipocytes may be reverting to preadipocyte-like precursor cells. Indeed, dedifferentiation and re-differentiation has been previously reported in mouse and rat adipocytes in several physiological and pathophysiological contexts such as pregnancy [186, 187], tissue repair [187] and tumorigenic transformations of liposarcomas [188]. In addition, dedifferentiation of visceral and subcutaneous mature adipocytes from individuals with obesity to fibroblast-like cells was previously shown to decrease mRNA expression of mature adipocyte gene markers including *PPARG2, C/EBPA, LPL* and adiponectin [189].

While this study currently focuses on the contribution of 14-3-3ζ to lipolysis, future experiments are aimed at understanding how 14-3-3ζ regulates other aspects of adipocyte function such as diet-induced obesity-mediated fat expansion. We previously reported that systemic 14-3-3ζ knockout mice displayed reduced adiposity and mild glucose intolerance compared to wild-type littermates under a high-fat diet [169]. In contrast, TAP mice overexpressing 14-3-3ζ gained more weight on a high-fat diet without displaying additional impairments in glucose tolerance or insulin sensitivity suggesting that 14-3-3ζ promotes adipose tissue expansion [169]. Thus, our prior observations suggest that adi14-3-3ζKO mice may gain less weight and display impaired glucose tolerance when challenged with a high-fat diet.

Collectively, results from our *in vivo* and *in vitro models* of decreased 14-3-3ζ function demonstrate that 14-3-3ζ facilitates lipolysis in a PKA-dependent manner and offer novel insights into the roles of 14-3-3 proteins in regulating lipid metabolism. In addition, our data also point to 14-3-3ζ acting as a central regulator of the development and maintenance of the mature adipocyte phenotype. This study complements our previous report of 14-3-3ζ being a mediator of adipogenesis [169]. Uncovering a regulatory role of 14-3-3ζ in lipolysis may lead to the development of new therapies aimed at targeting molecular scaffolds to treat conditions that result from dysregulated lipid metabolism.

2.6 Figures and Tables

Figure 1. Adipocyte-specific 14-3-3ζ knockout (adi14-3-3ζKO) mice do not display a metabolic phenotype. (A-B) Validation of adipocyte-specific deletion of *Ywhaz* (encoding 14-3-3ζ) in gonadal (gWAT), inguinal (iWAT) and brown (BAT) adipose depots of male (A) and female (B) adi14-3-3ζKO mice by qPCR (n=14 Cre+ wt, n=10 Cre+ fl/fl for male mice *: $p<0.05$ Cre+ fl/fl vs Cre+ wt mice; n=7 Cre+ wt, n=7 Cre+ fl/fl for female mice). **(C-D)** Body weights of male (C) and female (D) adi14-3-3ζKO mice following i.p injections of tamoxifen (50 mg/kg b.w) (n=14 Cre+ wt, n=10 Cre+ fl/fl for male mice; n=7 Cre+ wt, n=7 Cre+ fl/fl for female mice). **(E-F)** Intraperitoneal glucose (2 g/kg b.w.) tolerance tests on male (E) and female (F) adi14-3-3ζKO mice fasted for 6 hours at 12 weeks of age (n=9 Cre+ wt, n=6 Cre+ fl/fl for male mice; n=6 Cre+ wt, n=6 Cre+ fl/fl for female mice). **(G-H)** Intraperitoneal insulin (0.5 U/kg b.w.) tolerance tests on male (G) and female (H) adi14-3-3ζKO mice fasted for 4 hours at 13 weeks of age (n=6 Cre+ wt, n=6 Cre+ fl/fl for male mice; n=6 Cre+ wt, n=5 Cre+ fl/fl for female mice).

Figure 2. Lipolysis is impaired in adi14-3-3ζKO mice. (A-D) Plasma glycerol (A,B) and FFA (C,D) levels in male and female adi14-3-3ζKO mice injected with CL-316,243 (CL, 1 mg/kg b.w.) following an overnight fast (n=10 Cre+ wt, n=9 Cre+ fl/fl for male mice; n=7 Cre+ wt, n=7 Cre+ fl/fl for female mice; *: $p<0.05$ Cre+ fl/fl vs. Cre+ wt mice under the +CL condition. #: $p<0.05$ +CL vs. –CL for the same genotype). **(E-F)** Glycerol (E) and FFA (F) levels in the supernatant of male gonadal adipose tissue explants treated with isoproterenol (Iso, 1 µM) for 2 hours. Glycerol and FFA release were normalized to the mass of the explants (n=3-4 Cre+ wt, n=4-5 Cre+ fl/fl; *: $p<0.05$ Cre+ fl/fl vs. Cre+ wt mice under the +Iso condition. #: $p<0.05$ +Iso vs. –Iso for the same genotype).

Figure 3. Adipocyte-specific deletion of 14-3-3ζ impairs HSL activation in mice. (A-F) mRNA levels of *Atgl* (A-B)*, Hsl* (C-D)*,* and *Pparg* (E-F) in gonadal (gWAT) and inguinal (iWAT) adipose depots of male and female adi14-3-3ζKO mice (n=14 Cre+ wt, n=10 Cre+ fl/fl for male mice *: p<0.05 Cre+ fl/fl vs Cre+ wt mice; n=7 Cre+ wt, n=7 Cre+ fl/fl for female mice). **(G-H)** Immunoblot for phosphorylated and total levels of ATGL (G) and HSL (H) in gonadal adipose tissue (gWAT) of male adi14-3-3ζKO mice (n=6 per group).

Figure 4. Regulation of lipolysis by 14-3-3ζ occurs downstream of cAMP generation. (A-B) siRNA-mediated depletion of 14-3-3ζ in 3T3-L1 adipocytes transfected with scramble siRNA (siCon, 20 nM) or siRNA against 14-3-3ζ (siζ, 20 nM and 35 nM) was validated by qPCR (A) (n=6 per condition; *= p<0.05 siCon vs si14-3-3ζ) and immunoblotting of cell lysates for 14-3-3ζ (B) (n=3 per condition). **(C-D)** Levels of glycerol (C) and FFA (D) released by siRNA-transfected 3T3-L1 adipocytes (siCon, 20 nM or si14-3-3ζ, 35 nM) treated with isoproterenol (Iso, 1 μM), forskolin (10 μM) with IMBX (0.5 mM), or dibutyryl cAMP (dbcAMP, 1 mM) for 2 hours (n=6 per condition; *= p<0.05 siCon vs si14-3-3ζ). **(E-F)** mRNA levels of β-adrenergic receptor (E) and phosphodiesterase (F) isoforms in 14-3-3ζ-depleted 3T3-L1 adipocytes (n=6 per condition; *= p<0.05 siCon vs si14-3-3ζ). **(G)** Intracellular cAMP levels of siRNA-transfected 3T3-L1 lysates treated with Iso (1 μM) or forskolin (20 μM) for 1 hour (n=6-7 per condition). **(H)** mRNA expression of *Atgl* and *Hsl* lipases in 3T3-L1 cells following siRNA-mediated knockdown of 14-3-3ζ (n=6 per condition; *= p<0.05 siCon vs si14-3-3ζ). **(I)** Immunoblot for phosphorylated and total forms of HSL and CREB in siRNA-transfected 3T3-L1 lysates treated with Iso (1 μM), forskolin (10 μM) with IMBX (0.5 mM) or dbCAMP (1 mM) (n=6 per condition).

Figure 5. 14-3-3ζ depletion may alter adipocyte maturity. (A) mRNA levels of *Pparg, Fabp4, Fasn* and *Lpl* in 14-3-3ζ-depleted 3T3-L1 adipocytes (n=6 per condition for *Pparg*, *Fabp4, Fasn* and *Lpl;* *= p<0.05 siCon vs si14-3-3ζ). **(B)** Triacylglycerol content in siRNA-transfected mature 3T3-L1 adipocytes (n=6 per condition; *= p<0.05 siCon vs si14-3-3ζ, 1-tailed t-test). **(C-D)** Oil Red-O incorporation and quantification in 3T3-L1 adipocytes (C) and 4x magnification of cells (D) (n=4 per condition; *= p<0.05 siCon vs si14-3-3ζ).

Figure 6. Proposed regulatory role of 14-3-3ζ in lipolysis. Binding of an agonist to a β-adrenergic receptor activates adenylyl cyclase (AC) and increases cAMP production. cAMP activates PKA, which phosphorylates several substrates including the lipases ATGL, HSL and MAGL which catalyze the sequential conversion of triglycerides to glycerol and FFAs. The transcription factor CREB is also a PKA substrate. 14-3-3ζ has dual roles in lipolysis through facilitating the expression and activation of lipases and influencing cAMP-PKA-activity. Figure adapted from [190].

SUPPLEMENTARY FIGURES:

Figure S1. A-L The adipocyte-specific 14-3-3ζ KO (adi14-3-3ζKO) mouse model was validated by measuring mRNA levels of *Ywhab, Ywhag, Ywhae, Ywhah, Ywhas* and *Ywhaq* (encoding 14-3-3β, 14-3-3γ, 14-3-3ε, 14-3-3η, 14-3-3σ, and 14-3-3θ respectively) in gonadal (gWAT), inguinal (iWAT) and brown (BAT) adipose depots of male (**A-F**) and female (**G-L**) adi14-3-3ζKO mice (n=14 Cre+ wt, n=10 Cre+ fl/fl for male mice; n=7 Cre+ wt, n=7 Cre+ fl/fl for female mice).

Figure S2. siRNA-mediated knockdown of 14-3-3ζ was validated by measuring mRNA levels of *Ywhab, Ywhag, Ywhae, Ywhah, Ywhas* and *Ywhaq* (encoding 14-3-3β, 14-3-3γ, 14-3-3ε, 14-3-3η, 14-3-3σ, and 14-3-3θ respectively) in mature 3T3-L1 adipocytes transfected with scramble siRNA (siCon, 20 nM) or siRNA targeting 14-3-3ζ (si14-3-3ζ, 35 nM) (n=6 per condition).

Figure S3. (A) Validation immunoblot for 14-3-3ζ overexpression in 3T3-L1 adipocytes transfected with plasmids containing GFP (2 μg) or 14-3-3ζ IRES-GFP (2 μg) in the absence and presence of Iso (1 μM) for 2 hours (n=4 per condition). **(B)** FFA release from 14-3-3ζ-overexpressing 3T3-L1 adipocytes (n=4 per condition). *: $p<0.05$ GFP vs 14-3-3ζ IRES-GFP. **(C-F)** Plasma glycerol (C-D) and FFA (E-F) levels in male and female wild-type (WT) and 14-3-3ζ over-expressing (OE) transgenic mice injected intraperitoneally with Iso (10 mg/kg b.w.) following an overnight fast (n=5-6 WT, n=9-11 OE for male mice; n=8 WT, n=9-12 OE for female mice).

Supplementary Table 1. Primer sequences used for qPCR

Gene	Forward Sequence (5'-3')	Reverse Sequence (5'-3')
Ywhab	AATGCCACCCAGGCAGAAAGCA	CTTGGTAAGCCTGCTGGGAGTT
Ywhag	GGACTATTACCGTTACCTGGCAG	CTGCATGTGCTCCTTGCTGATC
Ywhae	CTAACACTGGCGAGTCCAAGGT	GTAAGCCACGAGGCTGTTCTCT
Ywhah	CCGCGTATAAGGAAGCCTTCGA	AGGCTTGCTCTGGTGCATTCTG
Ywhas	CATGAAGAGCGCCGTGGAAAAG	CTCTTCTGCTCGATGCTGGACA
Ywhaq	GCTGAAGTAGCTTGTGGCGATG	ATGCGTAGGCTGCATCTCCTTC
Ywhaz	CAGAAGACGGAAGGTGCTGAGA	CTTTCTGGTTGCGAAGCATTGGG
Hprt1	TCCTCCTCAGACCGCTTTT	CCTGGTTCATCATCGCTAATC
Adrb1	CTCGTCCGTCGTCTCCTTCTAC	GTCGATCTTCTTTACCTGTTTTTGG
Adrb2	TTGCAGTGGATCGCTATGTTG	TGACCACTCGGGCCTTATTCT
Adrb3	CCTTCAACCCGGTCATCTAC	GAAGATGGGGATCAAGCAAGC
Pde3b	CTTCACAAGGGATTGAGTGGCAGAACC	CATCCATGACTTGAAACACTGACTTCTTGG
Pde4a	TGGATGCCGTGTTCACAGACCTGG	GTTCTCAAGCACAGACTCATCGTTGTAC
Pde4b	CAGGAAAATGGTGATTGACATGGTGTTGG	CGAAGAACCTGTATCCGGTCAGTATAG
Pde4d	GGTCATTGACATTGTCCTGGCGACAG	CAGTGCACCATATTCTGAAGGACCTGG
Pparg	GGTCAGCTCTTGTGAATGGAA	ATCAGCTCTGTGGACCTCTCC
Fabp4	AGTACTCTCTGACCGGATGG	GGAAGCTTGTCTCCAGTGAA
Fasn	TGGGTTCTAGCCAGCAGAGT	ACCACCAGAGACCGTTATGC
Atgl	AACACCAGCATCCAGTTCAA	GGTTCAGTAGGCCATTCCTC
Hsl	ACCGAGACAGGCCTCAGTGTG	GAATCGGCCACCGGTAAAGAG
Magl	GTGCCTACCTGCTCATGGAAT	GAGGACGGAGTTGGTCACTTC
Lpl	GTGACCGATTTCATCAAGTTTGGAG	GACGGACACAAAGTTAGCACCAC

Supplementary Table 2. List of antibodies

Target	Host anti-species target	Dilution	Source	Product ID
14-3-3ζ	Rabbit	1:1000	Cell Signalling Technology	7413
Phosphorylated HSL (S660)	Rabbit	1:1000	Cell Signaling Technology	4126
Total HSL	Rabbit	1:1000	Cell Signaling Technology	4107
Phosphorylated CREB (S133)	Rabbit	1:1000	Cell Signaling Technology	9198
Total CREB	Rabbit	1:1000	ThermoFisher, Rockford, IL	MA1-083
ATGL	Rabbit	1:1000	Cell Signaling Technology	2439
PPARγ	Rabbit	1:1000	Cell Signaling Technology	2443
β-actin	Mouse	1:1000	Cell Signaling Technology	3700
β-tubulin	Mouse	1:1000	Cell Signaling Technology	86298
Anti-rabbit IgG HRP-linked antibody	Goat	1:2000	Cell Signaling Technology	7074
Anti-mouse IgG HRP-linked antibody	Horse	1:5000	Cell Signaling Technology	7076

Figure 1

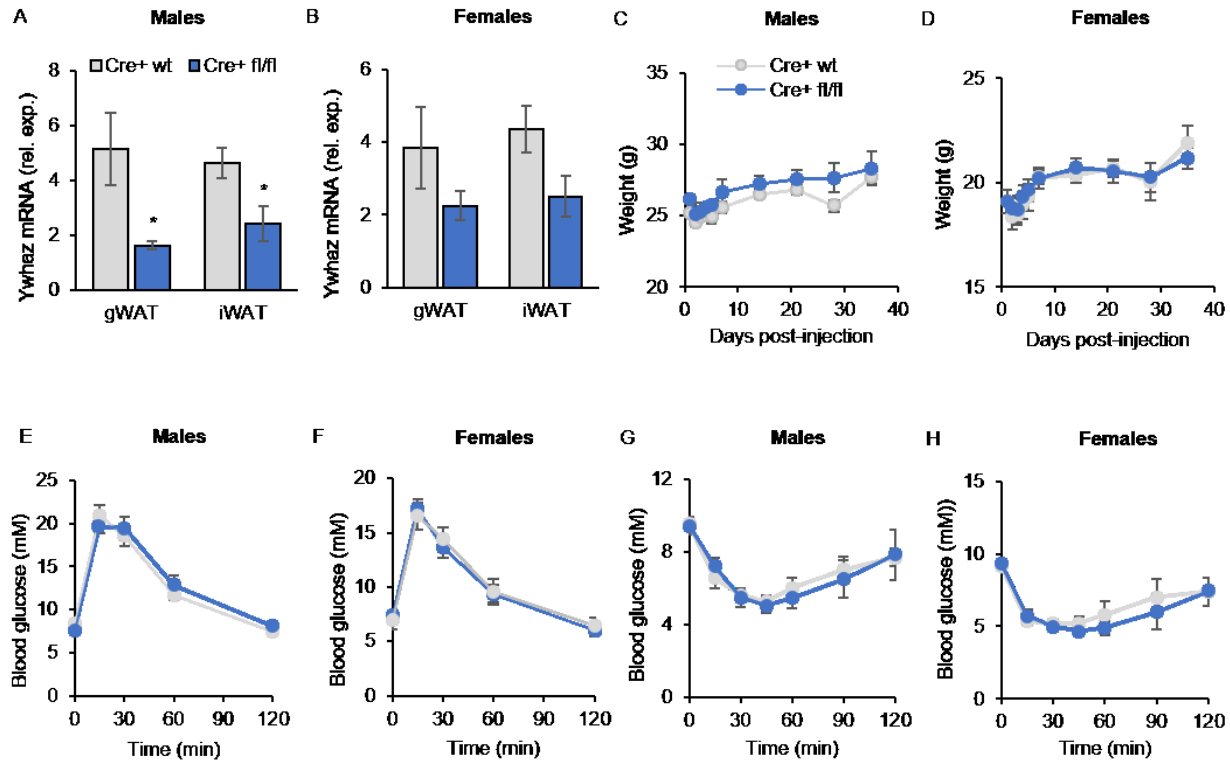
A
Males
Cre+ wt
Cre+ fl/fl
Ywhaz mRNA (rel. exp.)
gWAT
iWAT
B
Females
C
Males
Weight (g)
Days post-injection
D
Females
E
Males
Blood glucose (mM)
Time (min)
F
Females
G
Males
H
Females

Figure 2

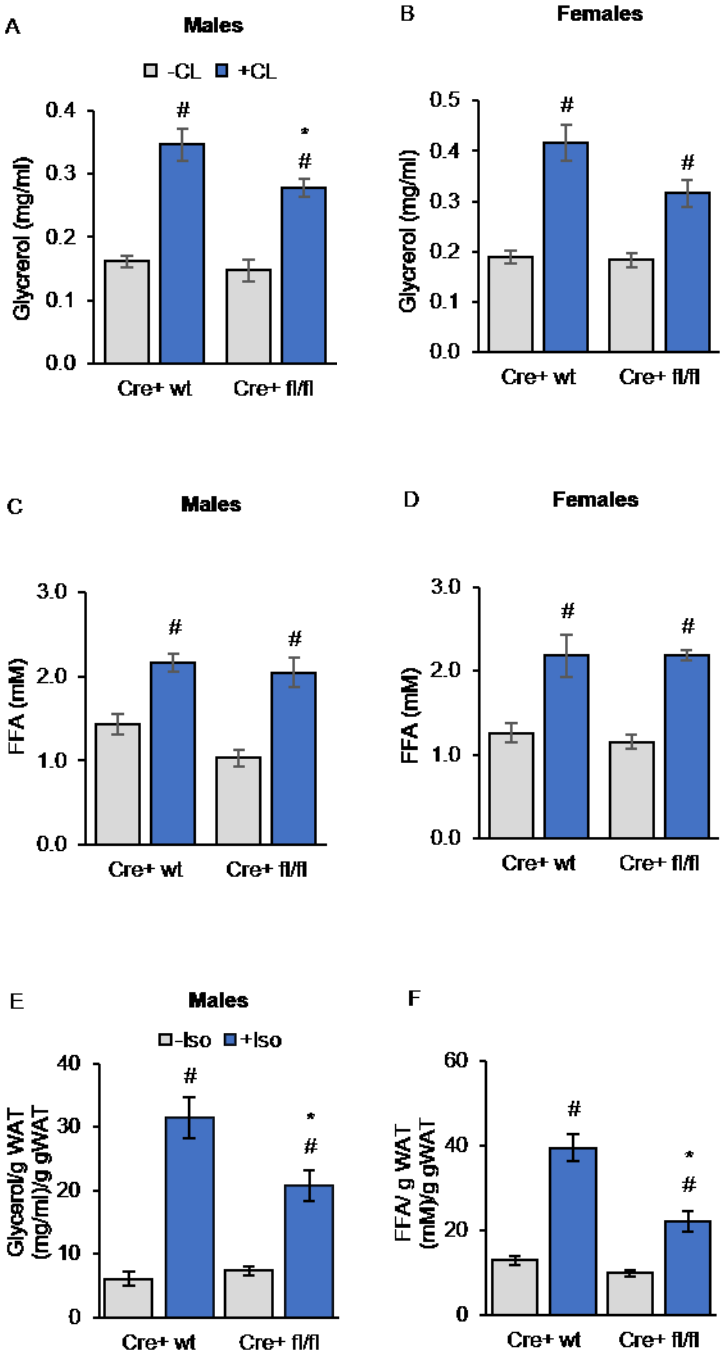
A
Males
-CL
+CL
Glycerol (mg/ml)
0.0
0.1
0.2
0.3
0.4
#
*
#
Cre+ wt
Cre+ fl/fl
B
Females
Glycerol (mg/ml)
0.0
0.1
0.2
0.3
0.4
0.5
#
#
Cre+ wt
Cre+ fl/fl
C
Males
FFA (mM)
0.0
1.0
2.0
3.0
#
#
Cre+ wt
Cre+ fl/fl
D
Females
FFA (mM)
0.0
1.0
2.0
3.0
#
#
Cre+ wt
Cre+ fl/fl
E
Males
-Iso
+Iso
Glycerol/g WAT (mg/ml)/g gWAT
0
10
20
30
40
#
*
#
Cre+ wt
Cre+ fl/fl
F
FFA/ g WAT (mM)/g gWAT
0
20
40
60
#
*
#
Cre+ wt
Cre+ fl/fl

Figure 3

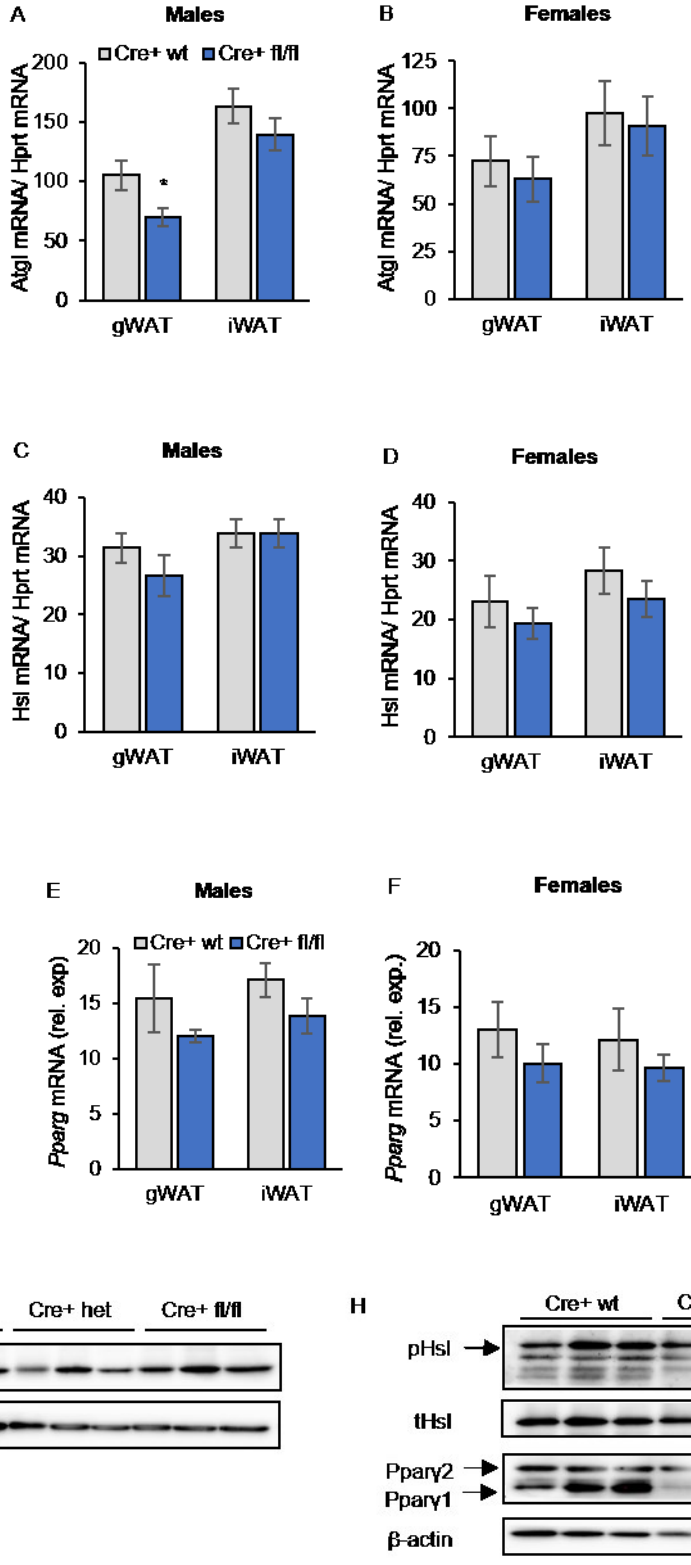
A
Males
Cre+ wt
Cre+ fl/fl
Atgl mRNA/ Hprt mRNA
200
150
100
50
0
*
gWAT
iWAT
B
Females
Atgl mRNA/ Hprt mRNA
125
100
75
50
25
0
gWAT
iWAT
C
Males
Hsl mRNA/ Hprt mRNA
40
30
20
10
0
gWAT
iWAT
D
Females
Hsl mRNA/ Hprt mRNA
40
30
20
10
0
gWAT
iWAT
E
Males
Cre+ wt
Cre+ fl/fl
Pparg mRNA (rel. exp)
20
15
10
5
0
gWAT
iWAT
F
Females
Pparg mRNA (rel. exp.)
20
15
10
5
0
gWAT
iWAT
G
Cre+ wt
Cre+ het
Cre+ fl/fl
Atgl
β-actin
H
Cre+ wt
Cre+ het
Cre+ fl/fl
pHsl
tHsl
Pparγ2
Pparγ1
β-actin

Figure 4

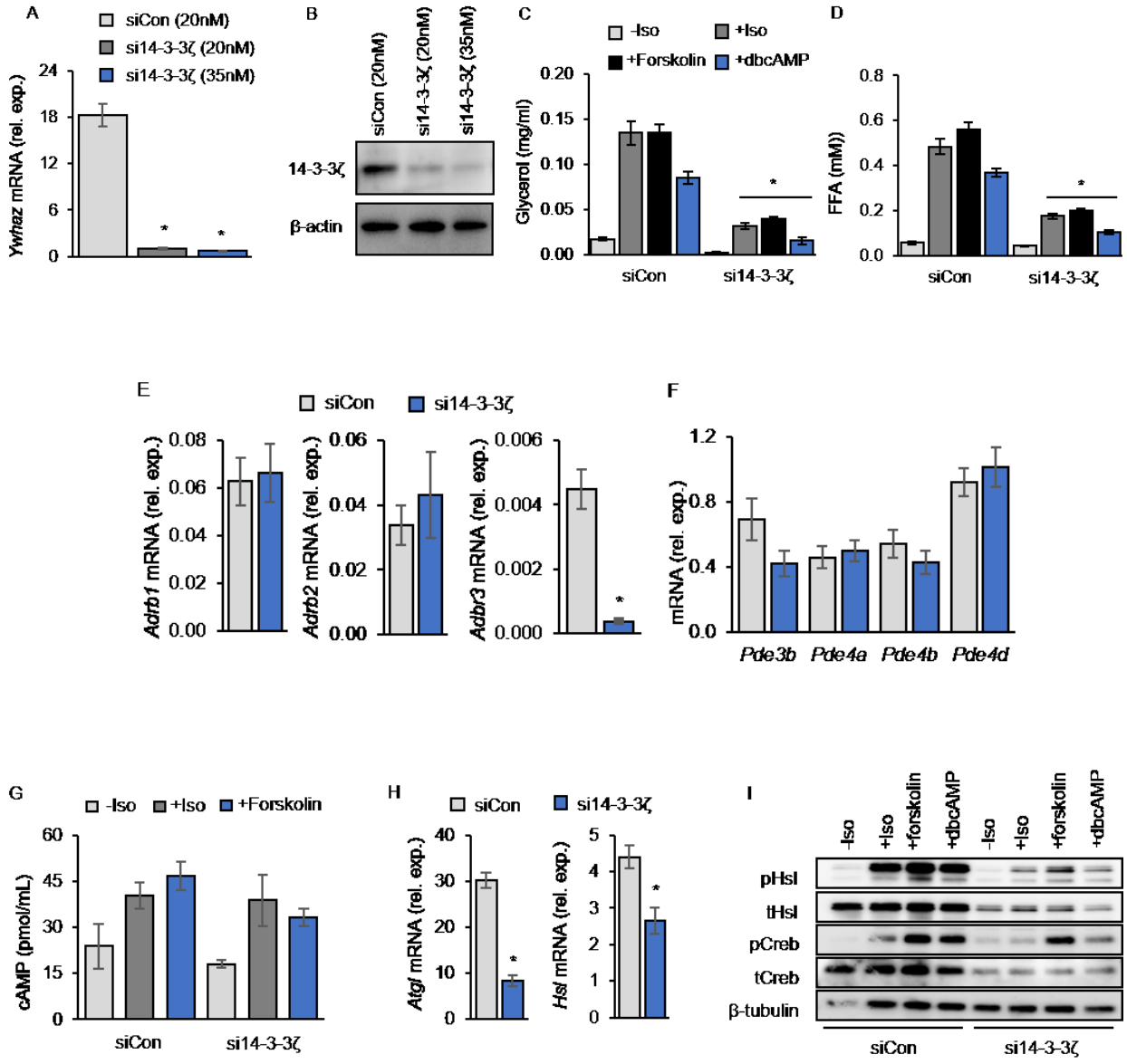
A
siCon (20nM)
si14-3-3ζ (20nM)
si14-3-3ζ (35nM)
Ywhaz mRNA (rel. exp.)
B
siCon (20nM)
si14-3-3ζ (20nM)
si14-3-3ζ (35nM)
14-3-3ζ
β-actin
C
-Iso
+Iso
+Forskolin
+dbcAMP
Glycerol (mg/ml)
siCon
si14-3-3ζ
D
FFA (mM))
siCon
si14-3-3ζ
E
siCon
si14-3-3ζ
Adrb1 mRNA (rel. exp.)
Adrb2 mRNA (rel. exp.)
Adbr3 mRNA (rel. exp.)
F
mRNA (rel. exp.)
Pde3b
Pde4a
Pde4b
Pde4d
G
-Iso
+Iso
+Forskolin
cAMP (pmol/mL)
siCon
si14-3-3ζ
H
siCon
si14-3-3ζ
Atgl mRNA (rel. exp.)
Hsl mRNA (rel. exp.)
I
-Iso
+Iso
+forskolin
+dbcAMP
-Iso
+Iso
+forskolin
+dbcAMP
pHsl
tHsl
pCreb
tCreb
β-tubulin
siCon
si14-3-3ζ

Figure 5

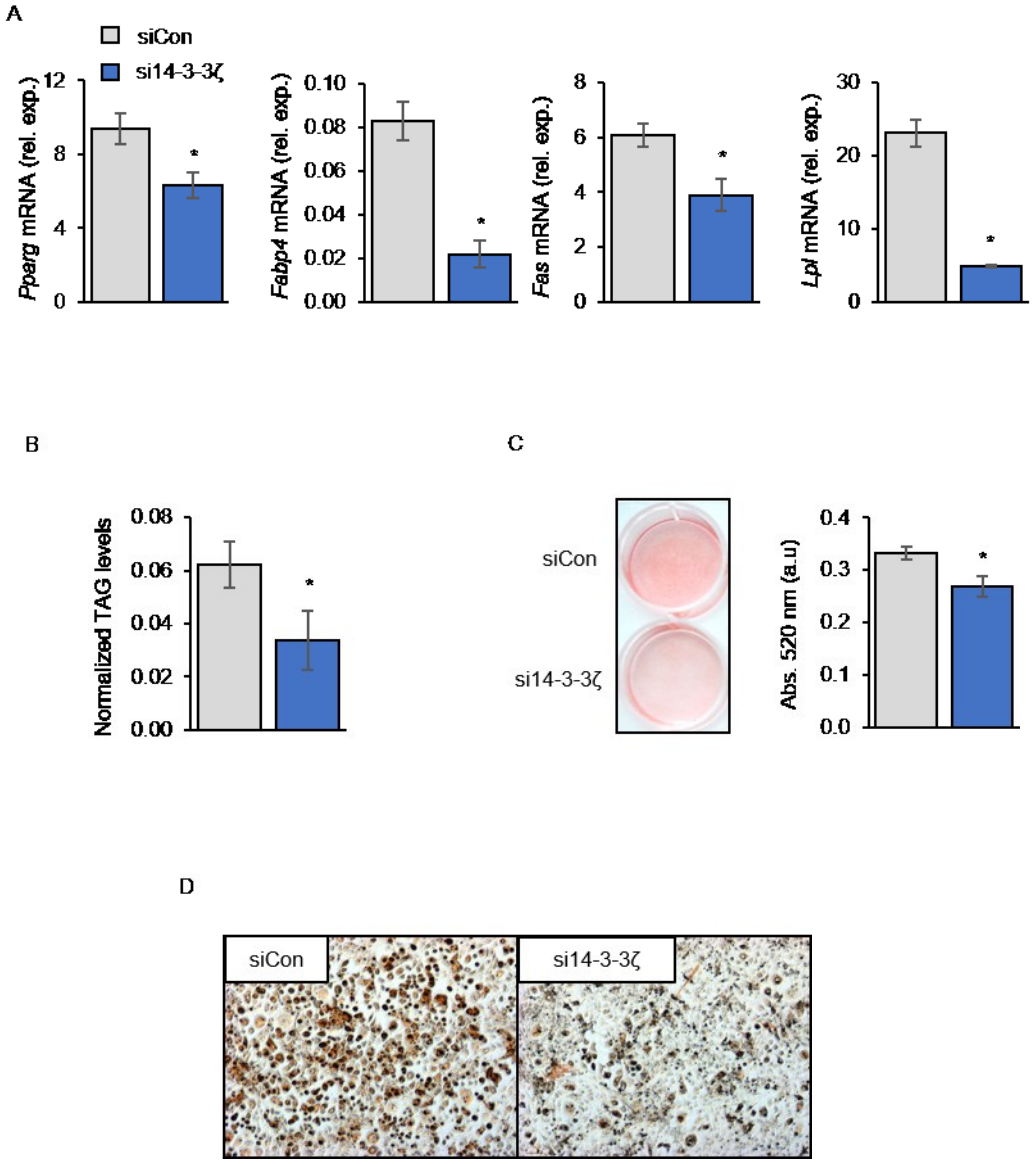
A
siCon
si14-3-3ζ
Pparg mRNA (rel. exp.)
Fabp4 mRNA (rel. exp.)
Fas mRNA (rel. exp.)
Lpl mRNA (rel. exp.)
B
Normalized TAG levels
C
siCon
si14-3-3ζ
Abs. 520 nm (a.u)
D
siCon
si14-3-3ζ

Figure 6

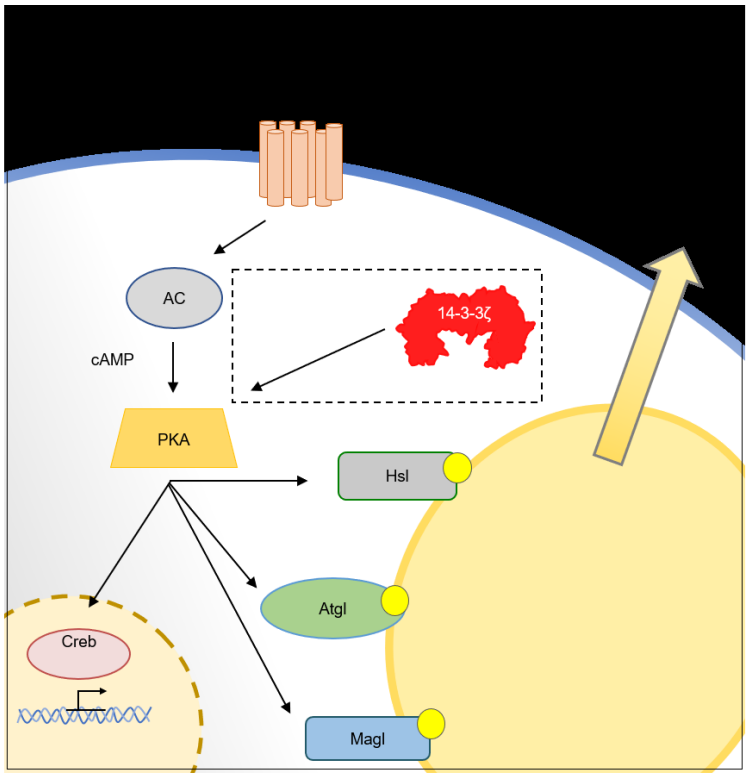

Figure S1

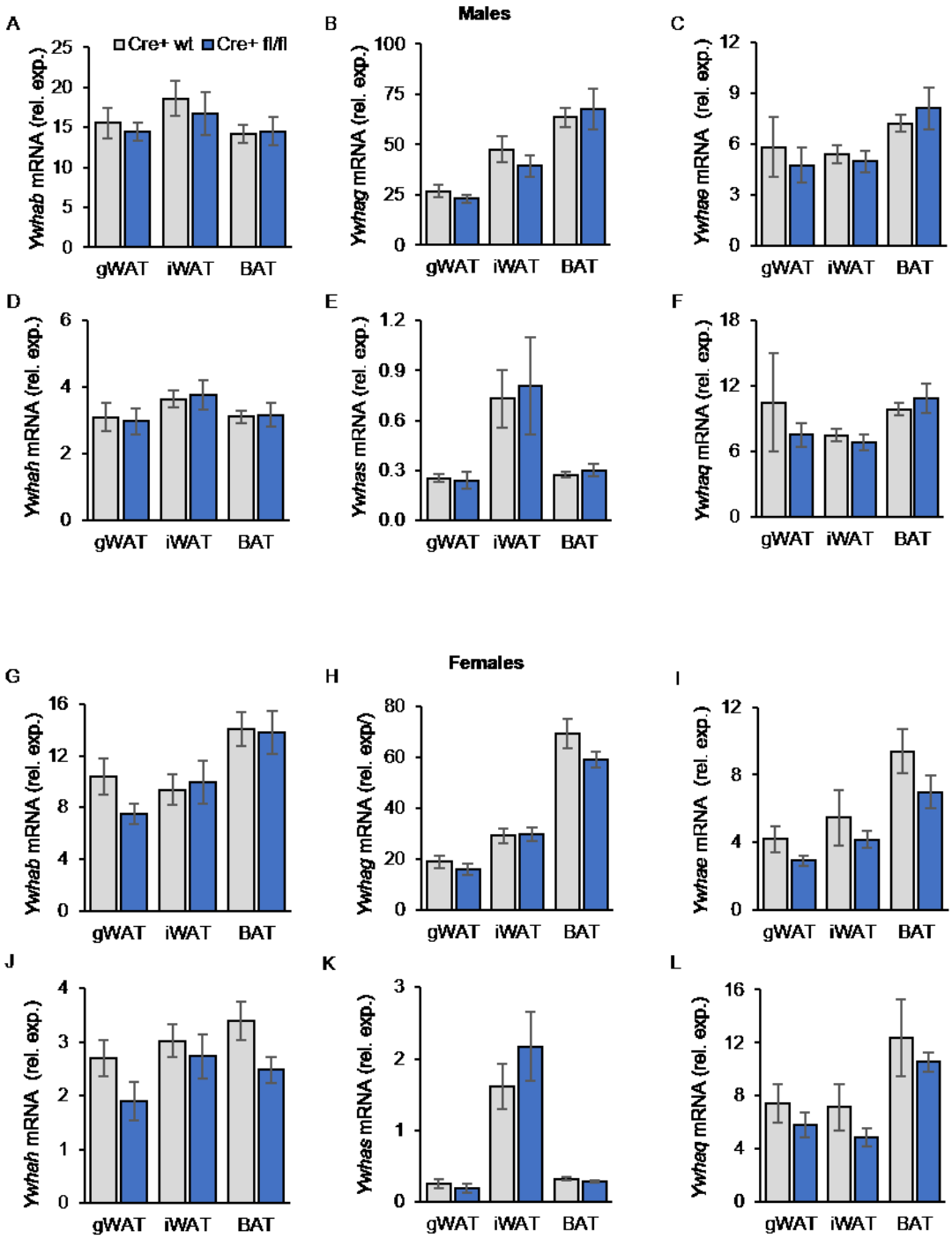
Males
Females
Cre+ wt
Cre+ fl/fl
A
B
C
D
E
F
G
H
I
J
K
L
Ywhab mRNA (rel. exp.)
Ywhag mRNA (rel. exp.)
Ywhae mRNA (rel. exp.)
Ywhah mRNA (rel. exp.)
Ywhas mRNA (rel. exp.)
Ywhaq mRNA (rel. exp.)
gWAT
iWAT
BAT

Figure S2

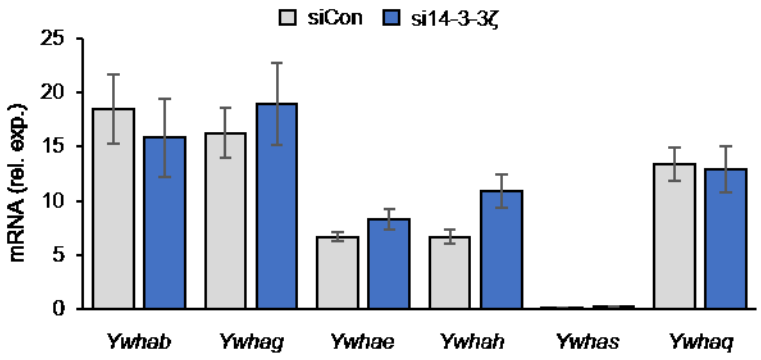
siCon
si14-3-3ζ
mRNA (rel. exp.)
25
20
15
10
5
0
Ywhab
Ywhag
Ywhae
Ywhah
Ywhas
Ywhaq

Figure S3

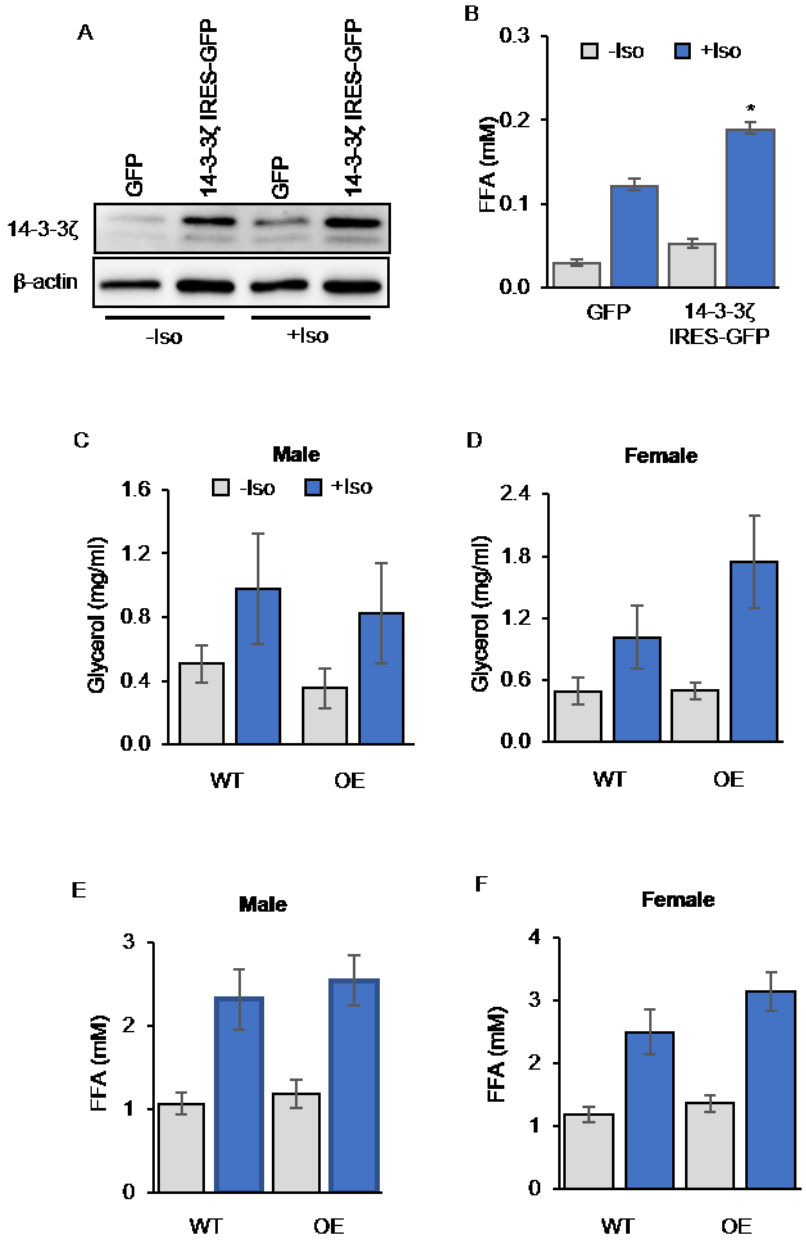
A
GFP
14-3-3ζ IRES-GFP
GFP
14-3-3ζ IRES-GFP
14-3-3ζ
β-actin
-Iso
+Iso
B
-Iso
+Iso
FFA (mM)
0.3
0.2
0.1
0.0
*
GFP
14-3-3ζ IRES-GFP
C
Male
-Iso
+Iso
Glycerol (mg/ml)
1.6
1.2
0.8
0.4
0.0
WT
OE
D
Female
Glycerol (mg/ml)
2.4
1.8
1.2
0.6
0.0
WT
OE
E
Male
FFA (mM)
3
2
1
0
WT
OE
F
Female
FFA (mM)
4
3
2
1
0
WT
OE

3.0 Discussion

The objective of this research project was to investigate the adipocyte-specific contributions of 14-3-3ζ to mature adipocyte function. White adipocytes specialize in both the storage and mobilization of energy that takes the form of lipids. During times in which the energy demand of other organs is high, WAT must hydrolyze triacylglycerols to generate FFAs which are then transported to the appropriate tissue for use as energy substrates [98]. Based on our previous findings of 14-3-3ζ being required for adipogenesis [169], we hypothesized that decreasing 14-3-3ζ expression in adipocytes would impair adipocyte-specific processes including lipolysis.

Whereas a significant reduction in plasma glycerol levels was detected in male adi14-3-3ζKO mice injected with CL-316,243 (Figure 2A), there was no difference in plasma FFA levels between the adi14-3-3ζKO and control groups (Figure 2C). This may possibly be explained by impaired FFA uptake by the BAT in adi14-3-3ζKO mice. The β3-adrenergic agonist CL-316,243 is known to stimulate lipolysis in white adipocytes, but its activation in BAT has been shown to induce BAT thermogenesis and FFA uptake [191-193]. Adipocyte-specific deletion of 14-3-3ζ could reduce FFA uptake by BAT, which when coupled to impaired lipolysis in WAT yields net plasma FFA levels that are comparable to plasma FFA levels measured in wild-type littermates. The rationale for reconciling the differences between the plasma glycerol and plasma FFA measurements is supported by the *ex vivo* lipolysis data that showed significant reductions in glycerol and FFA release in adi14-3-3ζKO gonadal explants that were isolated from other metabolically active tissues (Figures 2E and 2F). Measuring FFA uptake and FFA oxidation in BAT would address whether the plasma FFA measurements reflect altered BAT function.

The conclusion that 14-3-3ζ regulates lipolysis in a PKA-dependent manner was largely based on measurements of intracellular cAMP levels (Figure 4G) and immunoblotting of phosphorylated HSL and CREB (Figure 4I), which were indirect approaches to measure PKA activity. In the first case, significantly impaired glycerol and FFA release was observed in 14-3-3ζ-depleted 3T3-L1 adipocytes that had comparable cAMP levels to control-treated adipocytes. This suggests that impairment in the lipolysis

pathway occurs downstream of adenyl cyclase which generates cAMP. In the second case, PKA activity was measured in terms of phosphorylation of known PKA substrates. Additional studies are required to directly answer whether PKA activity is altered following the depletion of 14-3-3ζ. A co-immunoprecipitation experiment can address whether the regulation of lipolysis by 14-3-3ζ involves 14-3-3ζ interacting with PKA. This was done by Kent and colleagues who reported that 14-3-3γ and 14-3-3ε bind and regulate PKA activity to control neural outgrowth and growth cone turning responses [185]. Co-immunoprecipitation between HSL and 14-3-3ζ can also be performed to see whether regulation of lipolysis by 14-3-3ζ involves interactions with HSL. Alternatively, a pull-down assay which uses a bait protein instead of antibodies can be performed to assess whether 14-3-3ζ and PKA interact in a complex. It is also possible to measure PKA activity in cell homogenates with non-radioisotope kinase assays that use fluorescent-labelled phosphate acceptor peptides [194].

To confirm that regulation of lipolysis by 14-3-3ζ is PKA-dependent, a PKA overexpression-rescue experiment can be performed *in vitro*. This would require transfecting control and 14-3-3ζ-depleted 3T3-L1 adipocytes with plasmids encoding PKA. If knockdown of 14-3-3ζ impairs lipolysis by impairing PKA activity, then 14-3-3ζ-depleted 3T3-L1 cells overexpressing PKA will no longer exhibit decreased glycerol and FFA release as exogenous PKA compensates for the impaired activity of endogenous PKA. In addition, a mouse model whereby constitutively active PKA is specifically expressed in adipose tissue lacking 14-3-3ζ can be used to test whether 14-3-3ζ regulation of *in vivo* lipolysis is also PKA-dependent. In fact, a similar model was used by Kaihara et al. who reported that PKA activation enhanced acute-phase insulin secretion in β-cells [195].

Decreased markers of a mature adipocyte following 14-3-3ζ depletion suggests that adipocytes may be reverting to an immature state. Since there is not a complete absence of *Pparg* expression and lipid content, it is possible that some adipocytes may undergo a loss in adipocyte identity. As the expression of Cre is driven by the promoter of adiponectin, a mature adipocyte marker, recombination

only occurs in mature adipocytes of adi14-3-3ζKO mice. *In vivo* studies about the contribution of 14-3-3ζ to differentiation will require the *Pdgfrα*-Cre mouse line which is an ideal model for knockout studies in adipocyte precursor cells [196]. Additional characterization studies of the adi14-3-3ζKO mice are required to gain additional insights into the *in vivo* contributions of 14-3-3ζ in determining adipocyte maturity. gWAT and iWAT will be harvested to assay for TAG content to see if there is agreement between the *in vivo* and *in vitro* models. Histology analyses are also planned for harvested fat depots to see if size distribution is altered in the adipocytes of adi14-3-3ζKO mice. More specifically, these experiments would determine the contribution of 14-3-3ζ to adipocyte hypertrophy. Additional measurements for adipogenic markers such as angiotensin and resistin and preadipocyte markers including CD34, PDGFRα, PDGFRβ and PREF-1 [66] will provide additional insights into how 14-3-3ζ affects adipocyte maturity at the transcriptional level. If mature adipocytes are in fact reverting to a preadipocyte-like state, then one would expect reductions in angiotensin and resistin transcript levels and an increase in *CD34, Pdgfra, Pdgfrb,* and *Pref-1* mRNA levels.

As an organ specialized in the storage of energy, adipose tissue undergoes dynamic remodelling in response to changes in nutrient availability. This tightly regulated process requires coordination between adipocytes, stromal cells, macrophages, and extracellular matrix proteins [197, 198]. Although adipocyte-specific deletion of 14-3-3ζ was associated with impaired *in vivo* and *ex vivo* lipolysis, adi14-3-3ζKO mice did not display any differences in body weight or glucose metabolism under a normal chow diet (Figures 1C-H). Adi14-3-3ζKO mice will be placed on a high-fat diet to observe differences in body weight gain, fat mass, and adipocyte functions, such as adipokine secretion. Adi14-3-3ζKO mice may gain less weight and display impaired glucose tolerance and smaller WAT depots as reductions in PPARγ2 levels were observed in the gWAT. Indeed, multiple studies have shown that decreased PPARγ expression in mouse adipocytes impairs WAT and BAT formation and glucose tolerance [14, 15]. A high-fat diet study will also determine whether adi14-3-3ζKO mice may display impaired glucose tolerance,

which was our observation in a prior high-fat diet study involving systemic 14-3-3ζ knockout mice [169]. To address the impact of 14-3-3ζ overexpression in adipocytes, a doxycycline-inducible model may determine whether increasing levels of 14-3-3ζ in mice potentiates lipolysis and exacerbates weight gain. We predict that adipocyte-specific 14-3-3ζ-overexpressing mice will gain more weight that is independent of changes in glucose and insulin tolerance on a high-fat diet, as this phenotype was previously reported in the case of systemic overexpression of 14-3-3ζ [169, 199, 200].

WAT is not only considered as a storage site for lipids but is also an endocrine organ. WAT secretes a range of adipokines, such as leptin, adiponectin, VEGF and IL6 that have roles in regulating feeding behaviour, insulin sensitivity, angiogenesis in WAT and inflammation responses respectively [36, 37, 49, 66, 201]. ELISAs should also be performed to see whether any difference in serum adipokine levels between wild-type and knockout mice arises from a loss in the mature adipocyte phenotype.

A more in-depth analysis about the extent in which mature adipocyte function is altered by 14-3-3ζ deletion requires additional adipocyte processes to be examined, including lipogenesis, glucose uptake and fatty acid transport. Indeed, reductions in transcript levels were not seen only in *Pparg*, but also for *Fabp4* and *Fasn* which are important actors in fatty acid transport and *de novo* lipogenesis respectively. While the role of 14-3-3 proteins in fatty acid transport has not been studied in detail, reports have suggested that 14-3-3 proteins may have roles in *de novo* lipogenesis. In fact, FASN has been identified as a 14-3-3 binding partner in multiple affinity proteomic studies [180, 182]. Furthermore, the formation of a 14-3-3β – ChREBP complex was reported to involve 14-3-3β binding to the α2 helix of ChREBP [131]. This interface is in the N-terminal regulatory region of ChREBP that regulates its subcellular localization. Under low glucose or starvation conditions, 14-3-3β competes with importin-α (a protein that imports proteins into the nucleus) for binding to ChREBP and retains ChREBP in the cytosol thereby preventing the transcriptional activation of *de novo* lipogenesis genes [124, 132].

De novo lipogenesis can be examined by measuring the incorporation of labeled glucose into harvested fat pads for fatty acid synthesis [202].

In this study, acute deletion of 14-3-3ζ in fully developed adipose tissue did not affect body weight. However, the effects of adipocyte-specific 14-3-3ζ deletion during early adipose tissue development should be evaluated as subcutaneous depots develop during embryonic days 14-18 whereas gonadal depots develop postnatally [203, 204]. This temporal difference in the development of distinct depots requires the use of the *Pdgfra*-Cre and *Adipoq*-Cre constitutive knockout mouse lines, as 14-3-3ζ deletion targets adipocyte precursors cells in the former model and mature adipocytes in the latter [196].

Lastly, several studies have demonstrated that tamoxifen affects glucose tolerance and body weight in sex- and strain-dependent manners [200, 205]. Only mice that expressed Cre recombinase were used in this study, and all genotypes were injected with tamoxifen to account for any effects of Cre activation. The inclusion of Cre- wt and Cre- fl/fl mice as controls in this study would have addressed the specific effect of tamoxifen alone on glucose tolerance and insulin sensitivity. Nevertheless, deletion of 14-3-3ζ in adipocytes did not affect glucose tolerance in male and female mice, as adi14-3-3ζKO mice displayed virtually identical responses when challenged with intraperitoneal glucose and insulin. Moreover, no significant effects on body weight were observed after tamoxifen exposure.

4.0 Conclusion

In conclusion, our findings from our *in vitro* and *in vivo* models suggest that 14-3-3ζ contributes to the regulation of lipolysis in adipocytes. Adi14-3-3ζKO mice displayed impaired glycerol release, and gonadal adipose tissue explants displayed reductions in both glycerol and FFA release. *In vitro* lipolysis results were consistent with these findings as depletion of 14-3-3ζ in 3T3-L1 adipocytes using siRNA resulted in significant reductions in glycerol and FFA release in the supernatant. In addition, impaired HSL activation was observed in both models. Lastly, indicators of mature 14-3-3ζ-depleted adipocytes regressing to an immature state such as decreased transcript and protein levels of PPARγ and decreased lipid content suggest that 14-3-3ζ may have additional roles in determining adipocyte maturity. Future studies will address whether 14-3-3ζ contributes to other adipocyte-specific process that define the mature adipocyte.

5.0 Bibliography

1. Rosen, E.D. and O.A. MacDougald, *Adipocyte differentiation from the inside out.* Nat Rev Mol Cell Biol, 2006. **7**(12): p. 885-96.
2. Gustafson, B., et al., *Insulin resistance and impaired adipogenesis.* Trends Endocrinol Metab, 2015. **26**(4): p. 193-200.
3. Chen, Q., et al., *Fate decision of mesenchymal stem cells: adipocytes or osteoblasts?* Cell Death Differ, 2016. **23**(7): p. 1128-39.
4. Lefterova, M.I. and M.A. Lazar, *New developments in adipogenesis.* Trends Endocrinol Metab, 2009. **20**(3): p. 107-14.
5. Rosen, E.D. and B.M. Spiegelman, *What we talk about when we talk about fat.* Cell, 2014. **156**(1-2): p. 20-44.
6. Cristancho, A.G. and M.A. Lazar, *Forming functional fat: a growing understanding of adipocyte differentiation.* Nat Rev Mol Cell Biol, 2011. **12**(11): p. 722-34.
7. Tang, Q.Q., T.C. Otto, and M.D. Lane, *Commitment of C3H10T1/2 pluripotent stem cells to the adipocyte lineage.* Proc Natl Acad Sci U S A, 2004. **101**(26): p. 9607-11.
8. Jin, W., et al., *Schnurri-2 controls BMP-dependent adipogenesis via interaction with Smad proteins.* Dev Cell, 2006. **10**(4): p. 461-71.
9. Green, H. and M. Meuth, *An established pre-adipose cell line and its differentiation in culture.* Cell, 1974. **3**(2): p. 127-33.
10. Song, B.Q., et al., *Inhibition of Notch Signaling Promotes the Adipogenic Differentiation of Mesenchymal Stem Cells Through Autophagy Activation and PTEN-PI3K/AKT/mTOR Pathway.* Cell Physiol Biochem, 2015. **36**(5): p. 1991-2002.
11. Fontaine, C., et al., *Hedgehog signaling alters adipocyte maturation of human mesenchymal stem cells.* Stem Cells, 2008. **26**(4): p. 1037-46.
12. Tontonoz, P. and B.M. Spiegelman, *Fat and beyond: the diverse biology of PPARgamma.* Annu Rev Biochem, 2008. **77**: p. 289-312.
13. Barak, Y., et al., *PPAR gamma is required for placental, cardiac, and adipose tissue development.* Mol Cell, 1999. **4**(4): p. 585-95.
14. Koutnikova, H., et al., *Compensation by the muscle limits the metabolic consequences of lipodystrophy in PPAR gamma hypomorphic mice.* Proc Natl Acad Sci U S A, 2003. **100**(24): p. 14457-62.
15. Wang, F., et al., *Lipoatrophy and severe metabolic disturbance in mice with fat-specific deletion of PPARgamma.* Proc Natl Acad Sci U S A, 2013. **110**(46): p. 18656-61.
16. Tang, Q.Q., et al., *Sequential phosphorylation of CCAAT enhancer-binding protein beta by MAPK and glycogen synthase kinase 3beta is required for adipogenesis.* Proc Natl Acad Sci U S A, 2005. **102**(28): p. 9766-71.
17. MacDougald, O.A., et al., *Glucocorticoids reciprocally regulate expression of the CCAAT/enhancer-binding protein alpha and delta genes in 3T3-L1 adipocytes and white adipose tissue.* J Biol Chem, 1994. **269**(29): p. 19041-7.
18. Wu, Z., et al., *Conditional ectopic expression of C/EBP beta in NIH-3T3 cells induces PPAR gamma and stimulates adipogenesis.* Genes Dev, 1995. **9**(19): p. 2350-63.
19. Wu, Z., N.L. Bucher, and S.R. Farmer, *Induction of peroxisome proliferator-activated receptor gamma during the conversion of 3T3 fibroblasts into adipocytes is mediated by C/EBPbeta, C/EBPdelta, and glucocorticoids.* Mol Cell Biol, 1996. **16**(8): p. 4128-36.
20. Linhart, H.G., et al., *C/EBPalpha is required for differentiation of white, but not brown, adipose tissue.* Proc Natl Acad Sci U S A, 2001. **98**(22): p. 12532-7.
21. Tanaka, T., et al., *Defective adipocyte differentiation in mice lacking the C/EBPbeta and/or C/EBPdelta gene.* Embo j, 1997. **16**(24): p. 7432-43.

22. Oishi, Y., et al., *Kruppel-like transcription factor KLF5 is a key regulator of adipocyte differentiation.* Cell Metab, 2005. **1**(1): p. 27-39.
23. Hudak, C.S. and H.S. Sul, *Pref-1, a gatekeeper of adipogenesis.* Front Endocrinol (Lausanne), 2013. **4**: p. 79.
24. Banerjee, S.S., et al., *The Kruppel-like factor KLF2 inhibits peroxisome proliferator-activated receptor-gamma expression and adipogenesis.* J Biol Chem, 2003. **278**(4): p. 2581-4.
25. Kanazawa, A., et al., *Single nucleotide polymorphisms in the gene encoding Kruppel-like factor 7 are associated with type 2 diabetes.* Diabetologia, 2005. **48**(7): p. 1315-22.
26. Tong, Q., et al., *Interaction between GATA and the C/EBP family of transcription factors is critical in GATA-mediated suppression of adipocyte differentiation.* Mol Cell Biol, 2005. **25**(2): p. 706-15.
27. Seale, P., et al., *PRDM16 controls a brown fat/skeletal muscle switch.* Nature, 2008. **454**(7207): p. 961-7.
28. Kajimura, S., et al., *Regulation of the brown and white fat gene programs through a PRDM16/CtBP transcriptional complex.* Genes Dev, 2008. **22**(10): p. 1397-409.
29. Seale, P., et al., *Prdm16 determines the thermogenic program of subcutaneous white adipose tissue in mice.* J Clin Invest, 2011. **121**(1): p. 96-105.
30. Luong, Q., J. Huang, and K.Y. Lee, *Deciphering White Adipose Tissue Heterogeneity.* Biology (Basel), 2019. **8**(2).
31. Lee, M.J., Y. Wu, and S.K. Fried, *Adipose tissue heterogeneity: implication of depot differences in adipose tissue for obesity complications.* Mol Aspects Med, 2013. **34**(1): p. 1-11.
32. Chechi, K., W. van Marken Lichtenbelt, and D. Richard, *Brown and beige adipose tissues: phenotype and metabolic potential in mice and men.* J Appl Physiol (1985), 2018. **124**(2): p. 482-496.
33. Rosenwald, M., et al., *Bi-directional interconversion of brite and white adipocytes.* Nat Cell Biol, 2013. **15**(6): p. 659-67.
34. Zwick, R.K., et al., *Anatomical, Physiological, and Functional Diversity of Adipose Tissue.* Cell Metab, 2018. **27**(1): p. 68-83.
35. Kershaw, E.E. and J.S. Flier, *Adipose tissue as an endocrine organ.* J Clin Endocrinol Metab, 2004. **89**(6): p. 2548-56.
36. Friedman, J.M. and J.L. Halaas, *Leptin and the regulation of body weight in mammals.* Nature, 1998. **395**(6704): p. 763-70.
37. Ruan, H. and L.Q. Dong, *Adiponectin signaling and function in insulin target tissues.* J Mol Cell Biol, 2016. **8**(2): p. 101-9.
38. DeFronzo, R.A., et al., *Type 2 diabetes mellitus.* Nat Rev Dis Primers, 2015. **1**: p. 15019.
39. Schulz, T.J. and Y.H. Tseng, *Emerging role of bone morphogenetic proteins in adipogenesis and energy metabolism.* Cytokine Growth Factor Rev, 2009. **20**(5-6): p. 523-31.
40. Modica, S. and C. Wolfrum, *The dual role of BMP4 in adipogenesis and metabolism.* Adipocyte, 2017. **6**(2): p. 141-146.
41. Tseng, Y.H., et al., *New role of bone morphogenetic protein 7 in brown adipogenesis and energy expenditure.* Nature, 2008. **454**(7207): p. 1000-4.
42. Kim, H.J., et al., *Differential effects of interleukin-6 and -10 on skeletal muscle and liver insulin action in vivo.* Diabetes, 2004. **53**(4): p. 1060-7.
43. Mohamed-Ali, V., et al., *beta-Adrenergic regulation of IL-6 release from adipose tissue: in vivo and in vitro studies.* J Clin Endocrinol Metab, 2001. **86**(12): p. 5864-9.
44. Kanda, H., et al., *MCP-1 contributes to macrophage infiltration into adipose tissue, insulin resistance, and hepatic steatosis in obesity.* J Clin Invest, 2006. **116**(6): p. 1494-505.

45. Nugroho, D.B., et al., *Neuregulin-4 is an angiogenic factor that is critically involved in the maintenance of adipose tissue vasculature.* Biochem Biophys Res Commun, 2018. **503**(1): p. 378-384.
46. Pfeifer, A., *NRG4: an endocrine link between brown adipose tissue and liver.* Cell Metab, 2015. **21**(1): p. 13-4.
47. Steppan, C.M., et al., *Activation of SOCS-3 by resistin.* Mol Cell Biol, 2005. **25**(4): p. 1569-75.
48. Hotamisligil, G.S., et al., *Reduced tyrosine kinase activity of the insulin receptor in obesity-diabetes. Central role of tumor necrosis factor-alpha.* J Clin Invest, 1994. **94**(4): p. 1543-9.
49. Sung, H.K., et al., *Adipose vascular endothelial growth factor regulates metabolic homeostasis through angiogenesis.* Cell Metab, 2013. **17**(1): p. 61-72.
50. Ota, T., *Chemokine systems link obesity to insulin resistance.* Diabetes Metab J, 2013. **37**(3): p. 165-72.
51. Kosteli, A., et al., *Weight loss and lipolysis promote a dynamic immune response in murine adipose tissue.* J Clin Invest, 2010. **120**(10): p. 3466-79.
52. Nguyen, K.D., et al., *Alternatively activated macrophages produce catecholamines to sustain adaptive thermogenesis.* Nature, 2011. **480**(7375): p. 104-8.
53. Cherian, S., G.D. Lopaschuk, and E. Carvalho, *Cellular cross-talk between epicardial adipose tissue and myocardium in relation to the pathogenesis of cardiovascular disease.* Am J Physiol Endocrinol Metab, 2012. **303**(8): p. E937-49.
54. Rabe, K., et al., *Adipokines and insulin resistance.* Mol Med, 2008. **14**(11-12): p. 741-51.
55. Fazeli, P.K., et al., *Marrow fat and bone--new perspectives.* J Clin Endocrinol Metab, 2013. **98**(3): p. 935-45.
56. Hamrick, M.W., et al., *Leptin treatment induces loss of bone marrow adipocytes and increases bone formation in leptin-deficient ob/ob mice.* J Bone Miner Res, 2005. **20**(6): p. 994-1001.
57. Luo, X.H., et al., *Adiponectin stimulates RANKL and inhibits OPG expression in human osteoblasts through the MAPK signaling pathway.* J Bone Miner Res, 2006. **21**(10): p. 1648-56.
58. Ferron, M., et al., *Osteocalcin differentially regulates beta cell and adipocyte gene expression and affects the development of metabolic diseases in wild-type mice.* Proc Natl Acad Sci U S A, 2008. **105**(13): p. 5266-70.
59. Duong, M.N., et al., *The fat and the bad: Mature adipocytes, key actors in tumor progression and resistance.* Oncotarget, 2017. **8**(34): p. 57622-57641.
60. Bai, Y. and Q. Sun, *Macrophage recruitment in obese adipose tissue.* Obes Rev, 2015. **16**(2): p. 127-36.
61. Bartley, J.C., J.T. Emerman, and M.J. Bissell, *Metabolic cooperativity between epithelial cells and adipocytes of mice.* Am J Physiol, 1981. **241**(5): p. C204-8.
62. Hovey, R.C. and L. Aimo, *Diverse and active roles for adipocytes during mammary gland growth and function.* J Mammary Gland Biol Neoplasia, 2010. **15**(3): p. 279-90.
63. Inman, J.L., et al., *Mammary gland development: cell fate specification, stem cells and the microenvironment.* Development, 2015. **142**(6): p. 1028-42.
64. Cinti, S., *Pink Adipocytes.* Trends Endocrinol Metab, 2018. **29**(9): p. 651-666.
65. Rillema, J.A., *Development of the mammary gland and lactation.* Trends Endocrinol Metab, 1994. **5**(4): p. 149-54.
66. Wang, Q.A., et al., *Reversible De-differentiation of Mature White Adipocytes into Preadipocyte-like Precursors during Lactation.* Cell Metab, 2018. **28**(2): p. 282-288.e3.
67. Li, M., et al., *Mammary-derived signals activate programmed cell death during the first stage of mammary gland involution.* Proc Natl Acad Sci U S A, 1997. **94**(7): p. 3425-30.
68. Lund, L.R., et al., *Two distinct phases of apoptosis in mammary gland involution: proteinase-independent and -dependent pathways.* Development, 1996. **122**(1): p. 181-93.

69. Griffith, J.F., et al., *A study of bone marrow and subcutaneous fatty acid composition in subjects of varying bone mineral density.* Bone, 2009. **44**(6): p. 1092-6.
70. Devlin, M.J., et al., *Caloric restriction leads to high marrow adiposity and low bone mass in growing mice.* J Bone Miner Res, 2010. **25**(9): p. 2078-88.
71. Bathija, A., S. Davis, and S. Trubowitz, *Bone marrow adipose tissue: response to acute starvation.* Am J Hematol, 1979. **6**(3): p. 191-8.
72. Attané, C., et al., *Yellow adipocytes comprise a new adipocyte sub-type present in human bone marrow. BioRxiv [**preprint**]. May 19 2019. [cited 2019-07-31]. Available from https://doi.org/10.1101/641886*.
73. Park, A., W.K. Kim, and K.H. Bae, *Distinction of white, beige and brown adipocytes derived from mesenchymal stem cells.* World J Stem Cells, 2014. **6**(1): p. 33-42.
74. Frayn, K.N., *Visceral fat and insulin resistance--causative or correlative?* Br J Nutr, 2000. **83 Suppl 1**: p. S71-7.
75. Abate, N., et al., *Relationships of generalized and regional adiposity to insulin sensitivity in men.* J Clin Invest, 1995. **96**(1): p. 88-98.
76. Ibrahim, M.M., *Subcutaneous and visceral adipose tissue: structural and functional differences.* Obes Rev, 2010. **11**(1): p. 11-8.
77. Curat, C.A., et al., *Macrophages in human visceral adipose tissue: increased accumulation in obesity and a source of resistin and visfatin.* Diabetologia, 2006. **49**(4): p. 744-7.
78. Bruun, J.M., et al., *Monocyte chemoattractant protein-1 release is higher in visceral than subcutaneous human adipose tissue (AT): implication of macrophages resident in the AT.* J Clin Endocrinol Metab, 2005. **90**(4): p. 2282-9.
79. Karpe, F. and K.E. Pinnick, *Biology of upper-body and lower-body adipose tissue--link to whole-body phenotypes.* Nat Rev Endocrinol, 2015. **11**(2): p. 90-100.
80. Lepper, C. and C.M. Fan, *Inducible lineage tracing of Pax7-descendant cells reveals embryonic origin of adult satellite cells.* Genesis, 2010. **48**(7): p. 424-36.
81. Rodeheffer, M.S., K. Birsoy, and J.M. Friedman, *Identification of white adipocyte progenitor cells in vivo.* Cell, 2008. **135**(2): p. 240-9.
82. Berry, R. and M.S. Rodeheffer, *Characterization of the adipocyte cellular lineage in vivo.* Nat Cell Biol, 2013. **15**(3): p. 302-8.
83. Sebo, Z.L., et al., *A mesodermal fate map for adipose tissue.* Development, 2018. **145**(17).
84. Sanchez-Gurmaches, J. and D.A. Guertin, *Adipocytes arise from multiple lineages that are heterogeneously and dynamically distributed.* Nat Commun, 2014. **5**: p. 4099.
85. Merrick, D., et al., *Identification of a mesenchymal progenitor cell hierarchy in adipose tissue.* Science, 2019. **364**(6438).
86. Gliemann, J. and J. Vinten, *Lipogenesis and insulin sensitivity of single fat cells.* J Physiol, 1974. **236**(3): p. 499-516.
87. Varlamov, O., et al., *Cell-autonomous heterogeneity of nutrient uptake in white adipose tissue of rhesus macaques.* Endocrinology, 2015. **156**(1): p. 80-9.
88. Lee, K.Y., et al., *Developmental and functional heterogeneity of white adipocytes within a single fat depot.* EMBO J, 2019. **38**(3).
89. Bartz, R., et al., *Dynamic activity of lipid droplets: protein phosphorylation and GTP-mediated protein translocation.* J Proteome Res, 2007. **6**(8): p. 3256-65.
90. Welte, M.A., et al., *Developmental regulation of vesicle transport in Drosophila embryos: forces and kinetics.* Cell, 1998. **92**(4): p. 547-57.
91. Murphy, D.J., *The biogenesis and functions of lipid bodies in animals, plants and microorganisms.* Prog Lipid Res, 2001. **40**(5): p. 325-438.

92. Liu, P., et al., *Rab-regulated membrane traffic between adiposomes and multiple endomembrane systems.* Methods Enzymol, 2008. **439**: p. 327-37.
93. Zimmermann, R., et al., *Fate of fat: the role of adipose triglyceride lipase in lipolysis.* Biochim Biophys Acta, 2009. **1791**(6): p. 494-500.
94. Itabe, H., et al., *Perilipins: a diversity of intracellular lipid droplet proteins.* Lipids Health Dis, 2017. **16**(1): p. 83.
95. Brasaemle, D.L., et al., *Adipose differentiation-related protein is an ubiquitously expressed lipid storage droplet-associated protein.* J Lipid Res, 1997. **38**(11): p. 2249-63.
96. Jiang, H.P. and G. Serrero, *Isolation and characterization of a full-length cDNA coding for an adipose differentiation-related protein.* Proc Natl Acad Sci U S A, 1992. **89**(17): p. 7856-60.
97. Sztalryd, C., et al., *Functional compensation for adipose differentiation-related protein (ADFP) by Tip47 in an ADFP null embryonic cell line.* J Biol Chem, 2006. **281**(45): p. 34341-8.
98. Duncan, R.E., et al., *Regulation of lipolysis in adipocytes.* Annu Rev Nutr, 2007. **27**: p. 79-101.
99. Arner, P., *Catecholamine-induced lipolysis in obesity.* Int J Obes Relat Metab Disord, 1999. **23 Suppl 1**: p. 10-3.
100. Schweiger, M., et al., *Adipose triglyceride lipase and hormone-sensitive lipase are the major enzymes in adipose tissue triacylglycerol catabolism.* J Biol Chem, 2006. **281**(52): p. 40236-41.
101. Fredrikson, G., et al., *Hormone-sensitive lipase of rat adipose tissue. Purification and some properties.* J Biol Chem, 1981. **256**(12): p. 6311-20.
102. Yeaman, S.J., et al., *The multifunctional role of hormone-sensitive lipase in lipid metabolism.* Adv Enzyme Regul, 1994. **34**: p. 355-70.
103. Haemmerle, G., et al., *Hormone-sensitive lipase deficiency in mice causes diglyceride accumulation in adipose tissue, muscle, and testis.* J Biol Chem, 2002. **277**(7): p. 4806-15.
104. Holm, C., *Molecular mechanisms regulating hormone-sensitive lipase and lipolysis.* Biochem Soc Trans, 2003. **31**(Pt 6): p. 1120-4.
105. Anthonsen, M.W., et al., *Identification of novel phosphorylation sites in hormone-sensitive lipase that are phosphorylated in response to isoproterenol and govern activation properties in vitro.* J Biol Chem, 1998. **273**(1): p. 215-21.
106. Enoksson, S., et al., *Various phosphodiesterase subtypes mediate the in vivo antilipolytic effect of insulin on adipose tissue and skeletal muscle in man.* Diabetologia, 1998. **41**(5): p. 560-8.
107. Miyoshi, H., et al., *Perilipin promotes hormone-sensitive lipase-mediated adipocyte lipolysis via phosphorylation-dependent and -independent mechanisms.* J Biol Chem, 2006. **281**(23): p. 15837-44.
108. Zhang, H.H., et al., *Lipase-selective functional domains of perilipin A differentially regulate constitutive and protein kinase A-stimulated lipolysis.* J Biol Chem, 2003. **278**(51): p. 51535-42.
109. Zimmermann, R., et al., *Fat mobilization in adipose tissue is promoted by adipose triglyceride lipase.* Science, 2004. **306**(5700): p. 1383-6.
110. Steinberg, G.R., B.E. Kemp, and M.J. Watt, *Adipocyte triglyceride lipase expression in human obesity.* Am J Physiol Endocrinol Metab, 2007. **293**(4): p. E958-64.
111. Haemmerle, G., et al., *Defective lipolysis and altered energy metabolism in mice lacking adipose triglyceride lipase.* Science, 2006. **312**(5774): p. 734-7.
112. Ahmadian, M., et al., *Desnutrin/ATGL is regulated by AMPK and is required for a brown adipose phenotype.* Cell Metab, 2011. **13**(6): p. 739-48.
113. Pagnon, J., et al., *Identification and functional characterization of protein kinase A phosphorylation sites in the major lipolytic protein, adipose triglyceride lipase.* Endocrinology, 2012. **153**(9): p. 4278-89.
114. Lass, A., et al., *Adipose triglyceride lipase-mediated lipolysis of cellular fat stores is activated by CGI-58 and defective in Chanarin-Dorfman Syndrome.* Cell Metab, 2006. **3**(5): p. 309-19.

115. Granneman, J.G., et al., *Analysis of lipolytic protein trafficking and interactions in adipocytes.* J Biol Chem, 2007. **282**(8): p. 5726-35.
116. Miyoshi, H., et al., *Control of adipose triglyceride lipase action by serine 517 of perilipin A globally regulates protein kinase A-stimulated lipolysis in adipocytes.* J Biol Chem, 2007. **282**(2): p. 996-1002.
117. Vaughan, M., J.E. Berger, and D. Steinberg, *HORMONE-SENSITIVE LIPASE AND MONOGLYCERIDE LIPASE ACTIVITIES IN ADIPOSE TISSUE.* J Biol Chem, 1964. **239**: p. 401-9.
118. Sakurada, T. and A. Noma, *Subcellular localization and some properties of monoacylglycerol lipase in rat adipocytes.* J Biochem, 1981. **90**(5): p. 1413-9.
119. Zechner, R., et al., *Adipose triglyceride lipase and the lipolytic catabolism of cellular fat stores.* J Lipid Res, 2009. **50**(1): p. 3-21.
120. Taschler, U., et al., *Monoglyceride lipase deficiency in mice impairs lipolysis and attenuates diet-induced insulin resistance.* J Biol Chem, 2011. **286**(20): p. 17467-77.
121. Sugiura, T., et al., *2-Arachidonoylglycerol: a possible endogenous cannabinoid receptor ligand in brain.* Biochem Biophys Res Commun, 1995. **215**(1): p. 89-97.
122. Di Marzo, V. and I. Matias, *Endocannabinoid control of food intake and energy balance.* Nat Neurosci, 2005. **8**(5): p. 585-9.
123. Song, Z., A.M. Xiaoli, and F. Yang, *Regulation and Metabolic Significance of De Novo Lipogenesis in Adipose Tissues.* Nutrients, 2018. **10**(10).
124. Horton, J.D., J.L. Goldstein, and M.S. Brown, *SREBPs: activators of the complete program of cholesterol and fatty acid synthesis in the liver.* J Clin Invest, 2002. **109**(9): p. 1125-31.
125. Shao, W. and P.J. Espenshade, *Expanding roles for SREBP in metabolism.* Cell Metab, 2012. **16**(4): p. 414-9.
126. Matsuzaka, T. and H. Shimano, *Insulin-dependent and -independent regulation of sterol regulatory element-binding protein-1c.* J Diabetes Investig, 2013. **4**(5): p. 411-2.
127. Laplante, M. and D.M. Sabatini, *mTORC1 activates SREBP-1c and uncouples lipogenesis from gluconeogenesis.* Proc Natl Acad Sci U S A, 2010. **107**(8): p. 3281-2.
128. Shimano, H., et al., *Elevated levels of SREBP-2 and cholesterol synthesis in livers of mice homozygous for a targeted disruption of the SREBP-1 gene.* J Clin Invest, 1997. **100**(8): p. 2115-24.
129. Horton, J.D., et al., *Overexpression of sterol regulatory element-binding protein-1a in mouse adipose tissue produces adipocyte hypertrophy, increased fatty acid secretion, and fatty liver.* J Biol Chem, 2003. **278**(38): p. 36652-60.
130. Shimomura, I., et al., *Insulin resistance and diabetes mellitus in transgenic mice expressing nuclear SREBP-1c in adipose tissue: model for congenital generalized lipodystrophy.* Genes Dev, 1998. **12**(20): p. 3182-94.
131. Ge, Q., et al., *Structural characterization of a unique interface between carbohydrate response element-binding protein (ChREBP) and 14-3-3beta protein.* J Biol Chem, 2012. **287**(50): p. 41914-21.
132. Sakiyama, H., et al., *Regulation of nuclear import/export of carbohydrate response element-binding protein (ChREBP): interaction of an alpha-helix of ChREBP with the 14-3-3 proteins and regulation by phosphorylation.* J Biol Chem, 2008. **283**(36): p. 24899-908.
133. Iizuka, K. and Y. Horikawa, *ChREBP: a glucose-activated transcription factor involved in the development of metabolic syndrome.* Endocr J, 2008. **55**(4): p. 617-24.
134. Ortega-Prieto, P. and C. Postic, *Carbohydrate Sensing Through the Transcription Factor ChREBP.* Front Genet, 2019. **10**: p. 472.

135. Kawaguchi, T., et al., *Mechanism for fatty acid "sparing" effect on glucose-induced transcription: regulation of carbohydrate-responsive element-binding protein by AMP-activated protein kinase.* J Biol Chem, 2002. **277**(6): p. 3829-35.
136. Iizuka, K., et al., *Deficiency of carbohydrate response element-binding protein (ChREBP) reduces lipogenesis as well as glycolysis.* Proc Natl Acad Sci U S A, 2004. **101**(19): p. 7281-6.
137. Vijayakumar, A., et al., *Absence of Carbohydrate Response Element Binding Protein in Adipocytes Causes Systemic Insulin Resistance and Impairs Glucose Transport.* Cell Rep, 2017. **21**(4): p. 1021-1035.
138. Nuotio-Antar, A.M., et al., *FABP4-Cre Mediated Expression of Constitutively Active ChREBP Protects Against Obesity, Fatty Liver, and Insulin Resistance.* Endocrinology, 2015. **156**(11): p. 4020-32.
139. Abu-Elheiga, L., et al., *Human acetyl-CoA carboxylase 2. Molecular cloning, characterization, chromosomal mapping, and evidence for two isoforms.* J Biol Chem, 1997. **272**(16): p. 10669-77.
140. Mao, J., et al., *Liver-specific deletion of acetyl-CoA carboxylase 1 reduces hepatic triglyceride accumulation without affecting glucose homeostasis.* Proc Natl Acad Sci U S A, 2006. **103**(22): p. 8552-7.
141. Chirala, S.S. and S.J. Wakil, *Structure and function of animal fatty acid synthase.* Lipids, 2004. **39**(11): p. 1045-53.
142. Smith, S., A. Witkowski, and A.K. Joshi, *Structural and functional organization of the animal fatty acid synthase.* Prog Lipid Res, 2003. **42**(4): p. 289-317.
143. White, S.W., et al., *The structural biology of type II fatty acid biosynthesis.* Annu Rev Biochem, 2005. **74**: p. 791-831.
144. Chakravarthy, M.V., et al., *"New" hepatic fat activates PPARalpha to maintain glucose, lipid, and cholesterol homeostasis.* Cell Metab, 2005. **1**(5): p. 309-22.
145. Solinas, G., J. Boren, and A.G. Dulloo, *De novo lipogenesis in metabolic homeostasis: More friend than foe?* Mol Metab, 2015. **4**(5): p. 367-77.
146. Lodhi, I.J., et al., *Inhibiting adipose tissue lipogenesis reprograms thermogenesis and PPARgamma activation to decrease diet-induced obesity.* Cell Metab, 2012. **16**(2): p. 189-201.
147. Aitken, A., *14-3-3 proteins: a historic overview.* Semin Cancer Biol, 2006. **16**(3): p. 162-72.
148. Wang, W. and D.C. Shakes, *Molecular evolution of the 14-3-3 protein family.* J Mol Evol, 1996. **43**(4): p. 384-98.
149. Jones, D.H., S. Ley, and A. Aitken, *Isoforms of 14-3-3 protein can form homo- and heterodimers in vivo and in vitro: implications for function as adapter proteins.* FEBS Lett, 1995. **368**(1): p. 55-8.
150. Chaudhri, M., M. Scarabel, and A. Aitken, *Mammalian and yeast 14-3-3 isoforms form distinct patterns of dimers in vivo.* Biochem Biophys Res Commun, 2003. **300**(3): p. 679-85.
151. Liu, D., et al., *Crystal structure of the zeta isoform of the 14-3-3 protein.* Nature, 1995. **376**(6536): p. 191-4.
152. Xiao, B., et al., *Structure of a 14-3-3 protein and implications for coordination of multiple signalling pathways.* Nature, 1995. **376**(6536): p. 188-91.
153. Dougherty, M.K. and D.K. Morrison, *Unlocking the code of 14-3-3.* J Cell Sci, 2004. **117**(Pt 10): p. 1875-84.
154. Fu, H., R.R. Subramanian, and S.C. Masters, *14-3-3 proteins: structure, function, and regulation.* Annu Rev Pharmacol Toxicol, 2000. **40**: p. 617-47.
155. Muslin, A.J. and H. Xing, *14-3-3 proteins: regulation of subcellular localization by molecular interference.* Cell Signal, 2000. **12**(11-12): p. 703-9.
156. Kleppe, R., et al., *The 14-3-3 proteins in regulation of cellular metabolism.* Semin Cell Dev Biol, 2011. **22**(7): p. 713-9.

157. Van Der Hoeven, P.C., et al., *14-3-3 isotypes facilitate coupling of protein kinase C-zeta to Raf-1: negative regulation by 14-3-3 phosphorylation.* Biochem J, 2000. **345 Pt 2**: p. 297-306.
158. Van Schaftingen, E., L. Hue, and H.G. Hers, *Fructose 2,6-bisphosphate, the probably structure of the glucose- and glucagon-sensitive stimulator of phosphofructokinase.* Biochem J, 1980. **192**(3): p. 897-901.
159. Pozuelo Rubio, M., et al., *14-3-3s regulate fructose-2,6-bisphosphate levels by binding to PKB-phosphorylated cardiac fructose-2,6-bisphosphate kinase/phosphatase.* Embo j, 2003. **22**(14): p. 3514-23.
160. Bustos, D.M. and A.A. Iglesias, *A model for the interaction between plant GAPN and 14-3-3zeta using protein-protein docking calculations, electrostatic potentials and kinetics.* J Mol Graph Model, 2005. **23**(6): p. 490-502.
161. Piattoni, C.V., et al., *Nonphosphorylating glyceraldehyde-3-phosphate dehydrogenase is phosphorylated in wheat endosperm at serine-404 by an SNF1-related protein kinase allosterically inhibited by ribose-5-phosphate.* Plant Physiol, 2011. **156**(3): p. 1337-50.
162. Bustos, D.M. and A.A. Iglesias, *Phosphorylated non-phosphorylating glyceraldehyde-3-phosphate dehydrogenase from heterotrophic cells of wheat interacts with 14-3-3 proteins.* Plant Physiol, 2003. **133**(4): p. 2081-8.
163. Parker, L.L. and H. Piwnica-Worms, *Inactivation of the p34cdc2-cyclin B complex by the human WEE1 tyrosine kinase.* Science, 1992. **257**(5078): p. 1955-7.
164. Bridges, D. and G.B. Moorhead, *14-3-3 proteins: a number of functions for a numbered protein.* Sci STKE, 2005. **2005**(296): p. re10.
165. Hermeking, H., *The 14-3-3 cancer connection.* Nat Rev Cancer, 2003. **3**(12): p. 931-43.
166. Zha, J., et al., *Serine phosphorylation of death agonist BAD in response to survival factor results in binding to 14-3-3 not BCL-X(L).* Cell, 1996. **87**(4): p. 619-28.
167. Danial, N.N., et al., *Dual role of proapoptotic BAD in insulin secretion and beta cell survival.* Nat Med, 2008. **14**(2): p. 144-53.
168. Lim, G.E., et al., *Ywhaz/14-3-3zeta Deletion Improves Glucose Tolerance Through a GLP-1-Dependent Mechanism.* Endocrinology, 2016. **157**(7): p. 2649-59.
169. Lim, G.E., et al., *14-3-3zeta coordinates adipogenesis of visceral fat.* Nat Commun, 2015. **6**: p. 7671.
170. Mugabo, Y., et al., *Elucidation of the 14-3-3zeta interactome reveals critical roles of RNA-splicing factors during adipogenesis.* J Biol Chem, 2018. **293**(18): p. 6736-6750.
171. Ogihara, T., et al., *14-3-3 protein binds to insulin receptor substrate-1, one of the binding sites of which is in the phosphotyrosine binding domain.* J Biol Chem, 1997. **272**(40): p. 25267-74.
172. Ramm, G., et al., *A role for 14-3-3 in insulin-stimulated GLUT4 translocation through its interaction with the RabGAP AS160.* J Biol Chem, 2006. **281**(39): p. 29174-80.
173. Marvyn, P.M., et al., *Fasting upregulates adipose triglyceride lipase and hormone-sensitive lipase levels and phosphorylation in mouse kidney.* Biochem Cell Biol, 2015. **93**(3): p. 262-7.
174. Ferl, R.J., M.S. Manak, and M.F. Reyes, *The 14-3-3s.* Genome Biol, 2002. **3**(7): p. Reviews3010.
175. Mhawech, P., *14-3-3 proteins--an update.* Cell Res, 2005. **15**(4): p. 228-36.
176. Angrand, P.O., et al., *Transgenic mouse proteomics identifies new 14-3-3-associated proteins involved in cytoskeletal rearrangements and cell signaling.* Mol Cell Proteomics, 2006. **5**(12): p. 2211-27.
177. Sun, C., et al., *Adipose Snail1 Regulates Lipolysis and Lipid Partitioning by Suppressing Adipose Triacylglycerol Lipase Expression.* Cell Rep, 2016. **17**(8): p. 2015-2027.
178. Shi, H.B., et al., *Peroxisome proliferator-activated receptor gamma1 and gamma2 isoforms alter lipogenic gene networks in goat mammary epithelial cells to different extents.* J Dairy Sci, 2014. **97**(9): p. 5437-47.

179. Takenaka, A., et al., *Human-specific SNP in obesity genes, adrenergic receptor beta2 (ADRB2), Beta3 (ADRB3), and PPAR gamma2 (PPARG), during primate evolution.* PLoS One, 2012. **7**(8): p. e43461.
180. Meek, S.E., W.S. Lane, and H. Piwnica-Worms, *Comprehensive proteomic analysis of interphase and mitotic 14-3-3-binding proteins.* J Biol Chem, 2004. **279**(31): p. 32046-54.
181. Bunney, T.D., H.S. van Walraven, and A.H. de Boer, *14-3-3 protein is a regulator of the mitochondrial and chloroplast ATP synthase.* Proc Natl Acad Sci U S A, 2001. **98**(7): p. 4249-54.
182. Pozuelo Rubio, M., et al., *14-3-3-affinity purification of over 200 human phosphoproteins reveals new links to regulation of cellular metabolism, proliferation and trafficking.* Biochem J, 2004. **379**(Pt 2): p. 395-408.
183. Green, H. and O. Kehinde, *An established preadipose cell line and its differentiation in culture. II. Factors affecting the adipose conversion.* Cell, 1975. **5**(1): p. 19-27.
184. Ntambi, J.M. and K. Young-Cheul, *Adipocyte differentiation and gene expression.* J Nutr, 2000. **130**(12): p. 3122s-3126s.
185. Kent, C.B., et al., *14-3-3 proteins regulate protein kinase a activity to modulate growth cone turning responses.* J Neurosci, 2010. **30**(42): p. 14059-67.
186. Corsa, C.A.S. and O.A. MacDougald, *Cyclical Dedifferentiation and Redifferentiation of Mammary Adipocytes.* Cell Metab, 2018. **28**(2): p. 187-189.
187. Liao, Y., et al., *In vivo dedifferentiation of adult adipose cells.* PLoS One, 2015. **10**(4): p. e0125254.
188. Bi, P., et al., *Notch activation drives adipocyte dedifferentiation and tumorigenic transformation in mice.* J Exp Med, 2016. **213**(10): p. 2019-37.
189. Matsumoto, T., et al., *Mature adipocyte-derived dedifferentiated fat cells exhibit multilineage potential.* J Cell Physiol, 2008. **215**(1): p. 210-22.
190. Lim, G.E. and J.D. Johnson, *14-3-3zeta: A numbers game in adipocyte function?* Adipocyte, 2016. **5**(2): p. 232-7.
191. Himms-Hagen, J., et al., *Effect of CL-316,243, a thermogenic beta 3-agonist, on energy balance and brown and white adipose tissues in rats.* Am J Physiol, 1994. **266**(4 Pt 2): p. R1371-82.
192. Lowell, B.B. and J.S. Flier, *Brown adipose tissue, beta 3-adrenergic receptors, and obesity.* Annu Rev Med, 1997. **48**: p. 307-16.
193. Warner, A., et al., *Activation of beta3-adrenoceptors increases in vivo free fatty acid uptake and utilization in brown but not white fat depots in high-fat-fed rats.* Am J Physiol Endocrinol Metab, 2016. **311**(6): p. E901-e910.
194. MacAla, L.J., J.P. Hayslett, and J.I. Smallwood, *TECHNICAL NOTE: measurement of cAMP-dependent protein kinase activity using a fluorescent-labeled kemptide.* Kidney Int, 1998. **54**(5): p. 1746-50.
195. Kaihara, K.A., et al., *beta-Cell-specific protein kinase A activation enhances the efficiency of glucose control by increasing acute-phase insulin secretion.* Diabetes, 2013. **62**(5): p. 1527-36.
196. Jeffery, E., et al., *Characterization of Cre recombinase models for the study of adipose tissue.* Adipocyte, 2014. **3**(3): p. 206-11.
197. Choe, S.S., et al., *Adipose Tissue Remodeling: Its Role in Energy Metabolism and Metabolic Disorders.* Front Endocrinol (Lausanne), 2016. **7**: p. 30.
198. Martinez-Santibanez, G. and C.N. Lumeng, *Macrophages and the regulation of adipose tissue remodeling.* Annu Rev Nutr, 2014. **34**: p. 57-76.
199. Park, J., et al., *VEGF-A-Expressing Adipose Tissue Shows Rapid Beiging and Enhanced Survival After Transplantation and Confers IL-4-Independent Metabolic Improvements.* Diabetes, 2017. **66**(6): p. 1479-1490.

200. Ye, R., et al., *Impact of tamoxifen on adipocyte lineage tracing: Inducer of adipogenesis and prolonged nuclear translocation of Cre recombinase.* Mol Metab, 2015. **4**(11): p. 771-8.
201. Senn, J.J., et al., *Suppressor of cytokine signaling-3 (SOCS-3), a potential mediator of interleukin-6-dependent insulin resistance in hepatocytes.* J Biol Chem, 2003. **278**(16): p. 13740-6.
202. Herman, M.A., et al., *A novel ChREBP isoform in adipose tissue regulates systemic glucose metabolism.* Nature, 2012. **484**(7394): p. 333-8.
203. Han, J., et al., *The spatiotemporal development of adipose tissue.* Development, 2011. **138**(22): p. 5027-37.
204. Wang, Q.A., et al., *Tracking adipogenesis during white adipose tissue development, expansion and regeneration.* Nat Med, 2013. **19**(10): p. 1338-44.
205. Ceasrine, A.M., et al., *Tamoxifen Improves Glucose Tolerance in a Delivery-, Sex-, and Strain-Dependent Manner in Mice.* Endocrinology, 2019. **160**(4): p. 782-790.